Prostaglandin E_2 constrains systemic inflammation through an innate lymphoid cell–IL-22 axis

Rodger Duffin[1], Richard A. O'Connor[1], Siobhan Crittenden[1], Thorsten Forster[2], Cunjing Yu[1], Xiaozhong Zheng[1], Danielle Smyth[3]*, Calum T. Robb[1], Fiona Rossi[4], Christos Skouras[1], Shaohui Tang[5], James Richards[1], Antonella Pellicoro[1], Richard B. Weller[1], Richard M. Breyer[6], Damian J. Mole[1], John P. Iredale[1], Stephen M. Anderton[1], Shuh Narumiya[7,8], Rick M. Maizels[3]*, Peter Ghazal[2,9], Sarah E. Howie[1], Adriano G. Rossi[1], Chengcan Yao[1]†

1. MRC Centre for Inflammation Research, The University of Edinburgh Queen's Medical Research Institute, Edinburgh EH16 4TJ, United Kingdom
2. Division of Pathway Medicine, Edinburgh Infectious Diseases, The University of Edinburgh, Edinburgh EH16 4SB, United Kingdom
3. Institute for Immunology and Infection Research, The University of Edinburgh, Edinburgh EH9 3JT, United Kingdom
4. MRC Centre for Regenerative Medicine, The University of Edinburgh, Edinburgh EH16 4UU, United Kingdom
5. Department of Gastroenterology, First Affiliated Hospital of Jinan University, Guangzhou 510630, China
6. Department of Veterans Affairs, Tennessee Valley Health Authority, and Department of Medicine, Vanderbilt University Medical Center, Nashville, Tennessee, USA
7. Innovation Center for Immunoregulation Technologies and Drugs (AK project), Kyoto University Graduate School of Medicine, Kyoto 606-8501, Japan
8. Core Research for Evolutional Science and Technology (CREST), Japan Science and Technology Agency (JST), Tokyo 102-0075, Japan
9. SynthSys–Synthetic and Systems Biology, The University of Edinburgh, Edinburgh EH9 3JD, United Kingdom

*Present address: Institute of Infection, Immunity and Inflammation, College of Medical, Veterinary and Life Sciences, University of Glasgow, Glasgow G12 8TA

†Corresponding author. E-mail: Chengcan.Yao@ed.ac.uk

Systemic inflammation, resulting from massive release of pro-inflammatory molecules into the circulatory system, is a major risk factor for severe illness, but the precise mechanisms underlying its control are incompletely understood. We observed that prostaglandin E_2 (PGE_2) through its receptor EP4 is down-regulated in human systemic inflammatory disease. Mice with reduced PGE_2 synthesis develop systemic inflammation, associated with translocation of gut bacteria, which can be prevented by treating with EP4 agonists. Mechanistically, we demonstrate that PGE_2–EP4 signaling directly acts on type 3 innate lymphoid cells (ILCs), promoting their homeostasis and driving them to produce interleukin-22 (IL-22). Disruption of the ILC/IL-22 axis impairs PGE_2–mediated inhibition of systemic inflammation. Hence, PGE_2–EP4 signaling inhibits systemic inflammation through ILC/IL-22 axis–dependent protection of gut barrier dysfunction.

Systemic inflammation commonly develops from locally invasive infection, is characterized by dysregulation of the innate immune system and overproduction of pro-inflammatory cytokines and can result in severe critical illness (e.g., bacteremia, sepsis and septic shock) *(1,2)*. Despite much research on systemic inflammation, our understanding of the precise mechanisms for its control remains incomplete and represents an unmet clinical need *(1-3)*. Prostaglandins (PGs) are bioactive lipid mediators generated from arachidonic acid via the enzymatic activity of cyclooxygenases (COXs) *(4)*. PGs participate in the pathogenesis of inflammatory disease *(4,5)* and many inflammatory conditions are treated using non-steroidal anti-inflammatory drugs (NSAIDs) that inhibit PG synthesis by blocking COXs *(6)*. NSAID therapy is also thought to confer similar beneficial effects in treating severe inflammation, but large randomized controlled clinical trials have found that NSAIDs failed to reduce mortality in severe systemic inflammation *(7,8)*. More importantly, NSAIDs use during evolving bacterial infection is associated with more severe critical illness *(9-13)*. Therefore there is an imperative to define the paradoxical regulatory role of PGs in systemic inflammation *(14)*.

PGE_2 is one of the most abundantly produced PGs and modulates immune and inflammatory responses through its receptors (EP1 – 4) *(4)*. We performed a genome-wide gene expression analysis of whole blood samples from neonates with sepsis *(15)* and found that expression of *PTGES2* (encoding membrane-associated PGE synthase-2) and *PTGER4* (encoding EP4) were significantly diminished in the sepsis group compared with non-infected controls **(Fig. 1A)**. The reduced expression of *PTGES2* and *PTGER4* was associated with increased neutrophil blood count as a marker of inflammation **(Fig. 1B).** Down-regulation of *PTGER4* and *PTGS2* (encoding COX2) was similarly observed in patients suffering from systemic inflammatory response syndrome,

sepsis, septic shock or severe blunt trauma; but in contrast, expression of *HPGD* (encoding 15-PGDH which mediates PGE_2 degradation) in these patients was up-regulated compared to non-infected controls (**fig. S1**). Consistent with this, blood monocytes from patients with sepsis and septic shock produced less PGE_2 *(16).* Thus the PGE_2–EP4 pathway is down-regulated in human severe systemic inflammatory disease.

To understand the mechanism(s) whereby PGE_2 regulates systemic inflammation, we challenged wild-type (WT) C57BL/6 mice with lipopolysaccharide (LPS) to induce systemic inflammation after pre-treatment with indomethacin, which effectively suppresses PGE_2 production *(17,18).* Mice pre-treated with indomethacin developed an enhanced cytokine storm (e.g., tumor necrosis factor-α (TNF-α) and IL-6) (**Fig. 1C**) as well as other inflammatory signs in indomethacin-treated mice, e.g., splenomegaly (**Fig. 1D**), peritonitis characterized by accumulation of $CD11b^+Ly\text{-}6G^+$ neutrophils (**Fig. 1E),** and a low-grade hepatic inflammation as characterized by sinusoidal lymphocytosis and necrosis/inflammatory foci in the parenchyma (**Fig. 1F**). Furthermore, co-administration of an EP4 agonist almost completely diminished indomethacin-augmented systemic inflammation (**Fig. 1, G to I**). Thus PGE_2-EP4 signaling constrains LPS-induced systemic inflammation.

Besides the inflammatory markers described above, we also detected dissemination of gut bacteria into normally sterile tissues (e.g., liver) of indomethacin-treated, but not control, mice (**Fig. 2A**). The co-administration of EP4 agonist blocked the dissemination of bacteria to sterile tissues (**Fig. 2B**). Although pathogenic bacteria spread via the bloodstream usually cause severe systemic inflammation, gut leakage of commensal bacteria, especially in patients with damaged gut

epithelium or endothelium, may also trigger systemic inflammation. We therefore tested whether these disseminated bacteria contribute to indomethacin-augmented systemic inflammation by treating mice with indomethacin and antibiotics, known to effectively deplete gut bacteria *(19)*. Antibiotic therapy reduced indomethacin-facilitated systemic inflammation (**Fig. 2, C to F**). Indomethacin-dependent systemic inflammation was also observed in *Rag1*$^{-/-}$ mice (**fig. S2**), and this was again diminished by EP4 agonism (**Fig. 2, G to I**). Thus PGE_2-EP4 signaling prevents systemic inflammation independently of adaptive immune cells.

Given that IL-22 has recently been shown to inhibit inflammatory responses, particularly in the intestine *(19-22)*, we hypothesized that IL-22 may mediate PGE_2 control of systemic inflammation. To test this hypothesis, we first examined the effect of PGE_2 on IL-22 production. Mice treated with indomethacin reduced LPS–induced IL-22 production (**Fig. 3A**), which was mimicked by an EP4 antagonist **(Fig. 3B**). Thus PGE_2-EP4 signaling promotes IL-22 production *in vivo*. While LPS-induced systemic inflammation in WT mice was worsened and prevented by indomethacin and EP4 agonist, respectively (**Fig. 1, G to I**), both had little effects on LPS-induced inflammation in IL-22-deficient mice *(ref. 23)* (**Fig. S3**). Thus IL-22 is required for coupling PGE_2-EP4 signaling-dependent control of systemic inflammation. Furthermore, co-administration of recombinant IL-22 (rIL-22) reduced indomethacin–induced bacterial dissemination, which positively correlated with reduced systemic inflammation (**Fig. 3, C** to **E**), implying that IL-22 mediates PGE_2 suppression of gut bacterial dissemination and subsequent systemic inflammation.

As both PGE_2 and IL-22 can potentially protect the gut epithelial barrier *(17-22)*, we reasoned that inhibition of bacterial dissemination by PGE_2 may act through augmenting IL-22 action on gut

epithelial cells. We therefore examined gene expression related to barrier function in intestinal tissues. Indomethacin not only suppressed expression of IL-22 but also its receptors, i.e., *Il22ra1* (encoding IL-22Rα1) and *Il10rb* (encoding IL-10Rβ), and their suppression was prevented by rIL-22 (**Fig. 3F**), suggesting that PGE_2 may strengthen IL-22–IL-22R signaling in intestinal epithelial cells. Indeed, IL-22R–target genes such as *Reg3b*, *Reg3g*, *Fut2 (24)*, mucins and tight junctions were similarly down-regulated by indomethacin but rescued by rIL-22 (**Fig. 3G** and **fig. S4**). Expression of genes related to IL-22R signaling and barrier function inversely correlated with gut bacterial dissemination (**Fig. 3E**). Given the protective role of PGE_2 in acute colonic mucosal injury *(17)*, we proposed that this protection is mediated by IL-22. Indeed, indomethacin worsened dextran sulfate sodium (DSS)-induced colitis and this was rescued by rIL-22, which elicited significantly less colitis disease activity index measured by weight loss, diarrhea and rectal bleeding (**Fig. 3H-J**). Our results thus indicate an important role of PGE_2 in regulating the intestinal epithelial barrier function through innate IL-22 signaling.

Flow cytometric analysis showed that IL-22-producing cells were $CD45^{Low}$Lineage(Lin)$^-$ $CD90.2^+$RORγt(retinoid acid receptor-related orphan receptor gamma)$^+$CCR6(CC chemokine receptor 6)$^+$ type 3 innate lymphoid cells (ILC3s, *ref. 22*) in the gut and $CD45^+$Lineage$^-$ $CD90.2^+CD4^+$ ILC3s in the spleen (**fig. S5**). We wondered whether these cells are involved in EP4-dependent control of systemic inflammation. Although *Rag1*$^{-/-}$ mice co-treated with indomethacin and an EP4 agonist (i.e., lacking PG signaling except through EP4) did not develop systemic inflammation (**Fig. 2, G to I**), depletion of $CD90.2^+$ ILCs restored indomethacin-induced systemic inflammation in these mice (**Fig. 4A**). To address whether PGE_2–EP4 signaling specifically in ILCs controls systemic inflammation, we crossed CD90.2-Cre mice *(25)* with EP4-

floxed mice *(26)* to generate tamoxifen-induced selective down-regulation of EP4 in CD90.2^{+} cells (including T cells and ILCs) in heterozygous CD90.2^{Cre}EP4$^{fl/+}$ mice (**Fig. 4B**). CD90.2^{Cre}EP4$^{fl/+}$ mice produced less IL-22 in response to LPS, which was associated with augmentation of systemic inflammatory response, e.g., TNF-α production (**Fig. 4B**), while down-regulation of EP4 in T cells *(27)* affected neither IL-22 nor TNF-α production (**fig. S6**). These data demonstrate that PGE_2-EP4 signaling controls systemic inflammation, at least in part, through the regulation of ILC3s.

Next, we investigated the impact of PGE_2 on ILC3 maintenance. Indomethacin significantly diminished ILC3 numbers in the gut and spleen at the steady state (**Fig. 4C and fig. S7, A to C**). This reduction was prevented by an EP4 agonist and was mimicked by an EP4 antagonist (**Fig. 4C and fig. S7)**. Consistently, ILC3s express PGE_2 receptors with especially high expression levels of EP4 (**fig. S8**). Furthermore, indomethacin down-regulated Ki-67 expression and an EP4 agonist prevented this reduction in ILC3s (**Fig. 4D**), suggesting that PGE_2-EP4 signaling potentiates ILC3 proliferation. PGE_2-EP4 signaling also prevented ILC3 apoptosis *in vitro* but it had little effect on ILC3 apoptosis *in vivo* (**Fig. S9, A and B**). Moreover, down-regulation of EP4 in CD90.2^{+} ILCs not only decreased RORγt^{+} ILC3s but also weakened IL-7 responsiveness, e.g., Bcl-2 expression, in ILC3s (**Fig. S9C**). To further understand the effect of PGE_2 on ILC3s, we measured gene expression by quantitative polymerase chain reaction in Lin^{-}CD45^{low}CD90.2^{hi}KLRG1^{-}CCR6^{+} ILC3s sorted from small intestines of mice treated with indomethacin and EP4 agonist. PGE_2-EP4 signaling up-regulates many ILC3 signature genes including *Rorc*, *Il23r*, *Il1r1*, *Il22*, *Il17a*, *Lta*, *Ltb*, *Tnfsf11* and *Tnfsf4* as well as *Bcl2l1* (**Fig. 4E**).

We next asked whether and how PGE_2 regulates ILC3 function. PGE_2 promoted IL-23-driven IL-22 production by gut lamina propria leukocytes isolated from *Rag1*$^{-/-}$ mice *in vitro* (**Fig. 4, F and G**) and this was inhibited by indomethacin (**Fig. 4H**). PGE_2 also promoted IL-22 production from splenic $CD4^+$ ILC3s, which was mediated by EP2 and EP4 (**fig. S10, A to C**). More importantly, PGE_2 increased IL-23-driven IL-22 production from highly purified $CD45^+Lin^-CD90.2^+KLRG1^-CCR6^+$ ILC3s from intestines and $CD3^-CD11b^-CD11c^-CD4^+$ ILC3s from spleen or bone marrow (**Fig. 4I and fig. S10D**), suggesting a direct action of PGE_2 on ILC3s. In addition, PGE_2 also increased IL-22 production from ILC3s in response to IL-1β and IL-7 (**fig. S11**). PGE_2 activated cyclic adenosine monophosphate signaling in ILC3s and in turn enhanced IL-22 production (**Fig. 4J and fig. S12, A and B**). Moreover, PGE_2-augmented IL-22 production depended on the transcription factor signal transducer and activator of transcription 3, which is critical for IL-22 production by ILC3s *(28),* but not RORγt or Ahr (**fig. S12, C to E**). Altogether, these data demonstrate that PGE_2–EP4 signaling promotes ILC3 homeostasis and IL-22 production through promoting ILC3 proliferation and enhancing cytokine (e.g., IL-7, IL-23 and IL-1) responsiveness.

Finally, we questioned whether PGE_2 promotes IL-22 production from human ILC3s. To answer this, we sorted human $Lin^-CD161^+CD127^+CD117^+CRTH2^-$ ILC3s from periphery blood of healthy donors and cultured them with IL-2, IL-23 and IL-1β to induce IL-22 production. Addition of PGE_2 similarly up-regulated IL-22 production from sorted human ILC3s (**Fig. 4K)**. Moreover, expression of the human *IL22* gene in healthy individuals infused with a bacterial endotoxin *(ref. 29)* positively correlated with expression of *PTGS2* and *PTGES* (encoding mPGES-1) (**fig. S13**); two inducible enzymes that mediate PGE_2 synthesis *(4)*. Acute pancreatitis (AP) is a sterile initiator of systemic inflammation that results in multiple organ dysfunction where gut barrier injury is

central to the pathogenesis *(30)*. Given that IL-22 was protective in an animal model of AP *(31)*, we measured IL-22 levels in patients with AP. IL-22 concentrations in plasma were lower in patients with AP compared to healthy controls at the time of admission to hospital (**Fig. 4L)**, further confirming that the reduction of IL-22 signaling is associated with development of systemic inflammation.

In summary, we identify a physiological role of endogenous PGE_2–EP4 signaling in activating the ILC3/IL-22 axis, which functionally contributes to crosstalk between the innate immune system, gut epithelium and microflora, and subsequently constrains systemic inflammation (**fig. S14**). These findings provide valuable insight towards understanding how inactivation of COXs may be harmful in severe bacterial infection and inflammation *(32-34)* and advance a crucial cellular and molecular mechanism for a scenario in which maintaining or augmenting PGE_2 signaling, e.g., by inhibiting the PGE_2-degrading enzyme 15-PGDH, protects intestinal barrier injury and potentiates its repair and control of systemic inflammation *(35, 36).*

References and Notes

1. R.S. Hotchkiss, I.E. Karl, The pathophysiology and treatment of sepsis. *N. Engl. J. Med.* **3481,** 138-150 (2003).
2. S.P. LaRosa, S.M. Opal, Immune aspects of sepsis and hope for new therapeutics. *Curr. Infect. Dis. Rep.* **14,** 474-483 (2012).
3. J. Cohen, S. Opal, T. Calandra, Sepsis studies need new direction. *Lancet Infect. Dis.* **12,** 503-505 (2012).
4. T. Hirata, S. Narumiya, Prostanoids as regulators of innate and adaptive immunity. *Adv. Immunol.* **116,** 143-174 (2012).
5. E. Ricciotti, G.A. FitzGerald, Prostaglandins and inflammation. *Arterioscler. Thromb. Vasc. Biol.* **31,** 986-1000 (2011).
6. R.O. Day, Non-steroidal anti-inflammatory drugs (NSAIDs). *BMJ* **346,** f3195 (2013).
7. G.R. Bernard, *et al.*, The effects of ibuprofen on the physiology and survival of patients with sepsis. The ibuprofen study group. *N. Engl. J. Med.* **336,** 912-918 (1997).
8. M.T. Haupt, M.S. Jastremski, T.P. Clemmer, C.A. Metz, G.B. Goris, Effect of ibuprofen in patients with severe sepsis: a randomized, double-blind, multicenter study. The ibuprofen study group. *Crit. Care Med.* **19,** 1339-1347 (1991).
9. D.M. Aronoff, Cyclooxygenase inhibition in sepsis: is there life after death? *Mediat. Inflamm.* **2012,** 696897 (2012).
10. D.P. Eisen, Manifold beneficial effects of acetyl salicylic acid and non-steroidal anti-inflammatory drugs on sepsis. *Intensive Care Med.* **38,** 1249-1257 (2012).
11. D.L. Stevens, Could nonsteroidal anti-inflammatory drugs (NSAIDs) enhance the progression of bacterial infections to toxic shock syndrome? *Clin. Infect. Dis.* **21,** 977-980 (1995).

12. A. Legras, *et al.,* A multicentre case-control study of nonsteroidal anti-inflammatory drugs as a risk factor for severe sepsis and septic shock. *Crit. Care.* **13,** R43 (2009).

13. B.H. Lee, *et al.,* Association of body temperature and antipyretic treatments with mortality of critically ill patients with and without sepsis: multi-centered prospective observational study. *Crit. Care.* **16,** R33 (2012).

14. J.N. Fullerton, A.J. O'Brien, D.W. Gilroy, Lipid mediators in immune dysfunction after severe inflammation. *Trends. Immunol.* **35,** 12-21 (2014).

15. C.L. Smith, *et al.,* Identification of a human neonatal immune-metabolic network associated with bacterial infection. *Nat. Commun.* **5,** 4649 (2014).

16. M. Bruegel, *et al.,* Sepsis-associated changes of the arachidonic acid metabolism and their diagnostic potential in septic patients. *Crit. Care. Med.* **40,** 1478–1486 (2012).

17. K. Kabashima, *et al.,* The prostaglandin receptor EP4 suppresses colitis, mucosal damage and CD4 cell activation in the gut. *J. Clin. Invest.* **109,** 883–893 (2002).

18. T. Chinen, *et al.,* Prostaglandin E_2 and SOCS1 have a role in intestinal immune tolerance. *Nat. Commun.* **2,** 190 (2011).

19. G.F. Sonnenberg, *et al.,* Innate lymphoid cells promote anatomical containment of lymphoid-resident commensal bacteria. *Science* **336,** 1321-1325 (2012).

20. R., Sabat, W. Ouyang, K. Wolk, Therapeutic opportunities of the IL-22-IL-22R1 system. *Nat. Rev. Drug. Discov.* **13,** 21-38 (2014).

21. G.F., Sonnenberg, L.A. Fouser, D. Artis, Border patrol: regulation of immunity, inflammation and tissue homeostasis at barrier surfaces by IL-22. *Nat. Immunol.* **12,** 383-390 (2011).

22. G. Eberl, M. Colonna, J.P. Di Santo, A.N. McKenzie, Innate lymphoid cells: A new paradigm in immunology. *Science* **348,** aaa6566 (2015).

23. K. Kreymborg, *et al.,* IL-22 is expressed by Th17 cells in an IL-23-dependent fashion, but not required for the development of autoimmune encephalomyelitis. *J. Immunol.* **179,** 8098–8104 (2007).

24. Y. Goto, *et al.*, Innate lymphoid cells regulate intestinal epithelial cell glycosylation. *Science* **345,** 1254009 (2014).

25. B. Zonta, *et al.,* A critical Role for Neurofascin in regulating action potential Initiation through maintenance of the Axon Initial Segment. *Neuron* **69,** 945-956 (2011).

26. A. Schneider, *et al.*, Generation of a conditional allele of the mouse prostaglandin EP4 receptor. *Genesis* **40,** 7-14 (2004).

27. C. Yao, *et al.,* Prostaglandin E_2 promotes Th1 differentiation via synergistic amplification of IL-12 signalling by cAMP and PI3-kinase. *Nat. Commun.* **4**, 1685 (2013).

28. X. Guo, *et al.,* Induction of innate lymphoid cell-derived interleukin-22 by the transcription factor STAT3 mediates protection against intestinal infection. *Immunity* **40,** 25-39 (2014).

29. S.E. Calvano, *et al.,* A network-based analysis of systemic inflammation in humans. *Nature* **437,** 1032-1037 (2005).

30. J.E. Fishman, *et al.* The intestinal mucus layer is a critical component of the gut barrier that is damaged during acute pancreatitis. *Shock* **42,** 264-270 (2014).

31. D. Feng, *et al.* Interleukin-22 ameliorates cerulein-induced pancreatitis in mice by inhibiting the autophagic pathway. *Int. J. Biol. Sci.* **8,** 249-257 (2012).

32. B. Xiang, *et al*., Platelets protect from septic shock by inhibiting macrophage-dependent inflammation via the cyclooxygenase 1 signalling pathway. *Nat. Commun.* **4**, 2657 (2013).

33. L.E. Fredenburgh, *et al.*, Cyclooxygenase-2 deficiency leads to intestinal barrier dysfunction and increased mortality during polymicrobial sepsis. *J. Immunol.* **187,** 5255-5267 (2011).

34. S.M. Hamilton, C.R. Bayer, D.L. Stevens, A.E. Bryant, Effects of selective and nonselective nonsteroidal anti-inflammatory drugs on antibiotic efficacy of experimental group A streptococcal myonecrosis. *J. Infect. Dis.* **209,** 1429-1435 (2014).

35. Y. Zhang, *et al.*, Inhibition of the prostaglandin-degrading enzyme 15-PGDH potentiates tissue regeneration. *Science* **348**, aaa2340 (2015).

36. K. Németh, *et al.*, Bone marrow stromal cells attenuate sepsis via prostaglandin E_2-dependent reprogramming of host macrophages to increase their interleukin-10 production. *Nat. Med.* **15,** 42-49 (2009).

Acknowledgments. We thank J. Allen for critically reading and editing the manuscript; P.J. Brophy and D. Mahad for CD90.2(Thy1.2)-Cre mice; J.C. Renauld for IL-22-deficient mice; J. Pollard, P.J. Spence and J. Thompson for *Rag1*$^{-/-}$ mice; T. Walsh and J. Rennie for human blood samples; Y.X. Fu, X.G. Guo, D. Ruckerl, T. Kendall, J. Hu, Q. Huang, G.T. Ho for invaluable advice, excellent technical assistance and/or discussion; and S. Johnston and W. Ramsay for cell sorting and analysis. We thank the Wellcome Trust Clinical Research Facility staff and the Department of Surgery, NHS Lothian. IL-22-deficient mice are available from Jean-Ludwig Institute For Cancer Research under a material transfer agreement with Jean-Christophe Renauld. This work was supported in part by the University of Edinburgh start-up funding (C.Yao.), Wellcome Trust Institutional Strategic Support Fund (C.Yao, J.P.I., S.M.A), Medical Research Council (MRC) UK (J.P.I., S.M.A., R.D., A.G.R.), NIH (DK37097) and a VA Merit (1BX000616 to R.M.B.), Health Foundation/Academy of Medical Sciences (D.J.M), University of Edinburgh/GlaxoSmithKline DPAC collaboration (D.J.M.), Wellcome Trust Investigator Award (R.M.M., Ref 106122) and Rainin Trust (R.M.M. 13H6), Core Research for Evolutional Science and Technology (CREST) of Japan Science and Technology Agency (S.N.), and EU FP7 IAPP project ClouDx-I, Chief Scientists Office (ETM202) and BBSRC (BB/K091121/1 to P.G.). The data presented in this manuscript are tabulated in the main paper and the supplementary materials. The authors declare no financial conflicts of interest.

SUPPLEMENTARY MATERIALS

www.sciencemag.org/content/xxx/xxxx/xxx/suppl/DC1

Materials and Methods

Figs. S1 to S14

References (37–55)

Fig. 1. PGE_2–EP4 signaling controls LPS–induced systemic inflammation. (**A)** Gene expression of *PTGES2* and *PTGER4* in whole blood samples of neonates suffering from sepsis with confirmed bacterial infection (Red, n=27) and matched non-infection controls (Blue, n=35). Line graphs display gene expression (Log_2 scale) as probability density plots for both group samples. Non-parametric Wilcoxon-Rank-Sum tests (P_{diff}) were used to test for differential expression of a gene between infected and control neonates. Fligner-Killeen tests (P_{var}) were used to test if sepsis and control groups have substantively different inter-subject variation in gene expression levels. **(B)** Supervised heat map of clinical neutrophil counts and expression levels for *PTGES2* and *PTGER4* genes for non-infected healthy controls (n=12) and bacterially infected neonates (n=27). Colored scale bar is shown for neutrophil count or gene expression z-score transformed values, respectively. ***P<0.001 by non-parametric Spearman correlation test performed to analyze the negative association between *PTGES2* (r_s=-0.6111) or *PTGER4* (r_s=-0.6323) gene expression and blood neutrophil counts. **(C** to **F)** Serum levels of TNF-α and IL-6 (C), spleen size and weight (D), neutrophil counts in peritoneal cavity lavage (E) and liver histology (F) of WT C57BL/6 mice treated with indomethacin (Indo) or vehicle control (Veh) for 5 d followed by LPS challenge injection for another 2 (C, n=6 per group) or 24 h (D to F, n=8 per group). **(G** to **I)** Spleen weight (G), neutrophils (H) and serum levels of TNF-α and IL-6 (I) of WT C57BL/6 mice treated with indomethacin and agonists for EP2 or EP4 followed by LPS challenge for 24 (G and H) or 2 h (I). Data shown as means ± SEM are pooled from two independent experiments. Scale bar, 50 μm. *P<0.05, **P<0.01 by one-way ANOVA. NS, not significant; ND, not detected.

Fig. 2. PGE_2 control of systemic inflammation involves gut bacterial dissemination and acts independently of adaptive immune cells. (A) Colony forming units (CFU) present in liver homogenates from WT C57BL/6 mice (n=6) treated with indomethacin for 5 d followed by LPS challenge for another 24 h. **(B)** CFU present in liver homogenates from WT C57BL/6 mice treated with indomethacin plus administration of an EP4 agonist (n=6) or vehicle (n=8) for 5 d followed by LPS challenge for another 24 h. **(C** to **F)** Spleen size and weight (C), neutrophils (D), liver histology (E) and serum levels of TNF-α and IL-6 (F) of WT C57BL/6 mice (n=6 per group) treated with indomethacin and antibiotics (ABX) for 5 d followed by LPS challenge for another 24 (C to E) or 2 h (F). **(G** to **I)** TNF-α and IL-6 levels in serum (G) and peritoneal cavity lavage (H) and CFU present in liver homogenates (I) from *Rag1*$^{-/-}$ mice treated with indomethacin plus administration of an EP4 agonist or vehicle control (n=8 per group) for 4 d. Data shown as means ± SEM are pooled from two independent experiments. Scale bar, 50 μm. **P*<0.05, ***P*<0.01, ****P*<0.001 by two-way ANOVA (C, D and F) or Mann-Whitney test (G to I). ND, not detected.

Figure 3. IL-22 mediates PGE_2 protection against systemic inflammation and intestinal barrier injury. (A) Serum IL-22 levels of WT C57BL6 mice treated with indomethacin (Indo, n=6) or vehicle control (Veh, n=6) for 5 days followed by challenge with LPS or PBS for 2 h. **(B)** Serum IL-22 levels in WT C57BL/6 mice treated with an EP4 antagonist or vehicle (n=4 per group) in drinking water for 5 d followed by LPS challenge for another 2 h. **(C** to **G)** *Rag1*$^{-/-}$ mice were treated with vehicle (Veh, n=9) or indomethacin (Indo) plus administration of rIL-22 (n=10) or vehicle control PBS (n=10) for 4 d. (C) CFUs present in liver homogenates; (D) neutrophil counts; (E) correlation of liver CFU with systemic inflammation profile and expression profile of genes related to intestinal barrier function; (F and G) gene expression of IL-22 and its receptors (F) and antimicrobial peptides (G) in the terminal ileum. Expression was measured by real-time PCR, normalized to *Gapdh* gene and presented as relative expression (in Log_2 Fold Change) to the vehicle control group. (**H** to **J**) Change in body weight (H), disease activity index (I) and colon length (J) of WT C57BL/6 mice (n=10 per group) treated with 2% DSS and indomethacin or vehicle control in drinking water plus administration of rIL-22 or vehicle control PBS for 6 days. Data shown as means ± SEM are pooled from two (A, H, I and J) or three (C to G) independent experiments or represent one experiment (B). **P*<0.05, ***P*<0.01, ****P*<0.001 by Mann-Whitney test (A, B and D), one-way ANOVA (C, F to J) or two-tailed Pearson correlation test (E).

Fig. 4. PGE_2–EP4 signaling potentiates ILC3 homeostasis and function that contributes to control of systemic inflammatory response. (A) Splenic CD90.2$^+$ ILCs, serum TNF-α levels in and neutrophil counts in *Rag1*$^{-/-}$ mice co-treated with indomethacin and an EP4 agonist plus anti-CD90.2 (αCD90.2) or control IgG antibodies (n=8 per group) for 4 days. **(B)** Expression of *Ptger4* mRNA in splenic CD90.2$^+$ cells and serum levels of IL-22 and TNF-α in tamoxifen-treated CD90.2^{Cre}EP4$^{fl/+}$ mice (n=7) and control C57BL/6 mice (n=5) at 1.5 h after LPS challenge. **(C-E)** *Rag1*$^{-/-}$ (C,D) or C57BL/6 (E) mice were treated with indomethacin with or without an EP4 agonist for 4-5 d. (**C**) Percentages and numbers of ILC3s in small intestines. Cells were *ex vivo* stimulated with IL-23 for 3 h. Each point represents an individual mouse. **(D)** Ki-67 expression in gut ILC3s. Each point represents an individual mouse. **(E)** Gene expression profile in gut ILC3s presented as relative expression to the vehicle control group. Data are the summary of two independent experiments with 8 mice for each group. **(F)** Expression of RORγt and IL-22 by *Rag1*$^{-/-}$ gut CD45$^+$ lamina propria leukocytes (LPLs) stimulated with IL-23 and PGE_2 for 4 h. Numbers in brackets represent IL-22 MFI of the RORγt$^+$IL-22$^+$ populations. **(G** to **J)** IL-22 production in supernatants by LPLs or ILC3s isolated from small intestines of *Rag1*$^{-/-}$ mice and then cultured with indicated conditions overnight (G, H, J) or for 3 d (I). **(K)** IL-22 production by human ILC3s cultured with IL-2, IL-23, IL-1β and PGE_2 for 4 d (n=5 donors). **(L)** Plasma IL-22 levels in individuals with acute pancreatitis (AP) at the time of presentation to hospital (n=48) or from healthy individual donors (n=28). Horizon line represent the mean for each group. Data shown as means ± SEM are pooled from two or more independent experiments (A, C to E, G, J and K) or represent one (B) or two (F, H, I) independent experiments. **P*<0.05, ***P*<0.01, ****P*<0.001 by unpaired Student's *t*-test (A, B, H and I), one-way ANOVA (C, D, F, G and J), ratio paired *t*-test (K) or Mann Whitney test (L).

Supplementary Materials for

Prostaglandin E_2 constrains systemic inflammation through an innate lymphoid cell–IL-22 axis

Rodger Duffin, Richard A. O'Connor, Siobhan Crittenden, Thorsten Forster, Cunjing Yu, Xiaozhong Zheng, Danielle Smyth, Calum T. Robb, Fiona Rossi, Christos Skouras, Shaohui Tang, James Richards, Antonella Pellicoro, Richard B. Weller, Richard M. Breyer, Damian J. Mole, John P. Iredale, Stephen M. Anderton, Shuh Narumiya, Rick M. Maizels, Peter Ghazal, Sarah E. Howie, Adriano G. Rossi, Chengcan Yao*

*Corresponding author. E-mail: Chengcan.Yao@ed.ac.uk

Published XX XX 2016, Science XXX, XXX (2016)
DOI: 10.1126/science.aad9903

This PDF file includes:

Materials and Methods

Mice.

Wild-type C57BL/6 mice were purchased from Harlan UK. To generate mice with selective EP4 deficiency in CD90.2^{+} ILCs, CD90.2(Thy1.2)-Cre mice on C57BL/6 background *(25)* were crossed to lox-flanked *Ptger4* (EP4-floxed) mice on C57BL/6 background *(26)*. EP4-floxed mice were also crossed with Lck-Cre mice (on C57BL/6 background) to generate mice with selective EP4 deletion in T cells *(27)*. All gene-modified mice including C57BL/6 *Rag1*$^{-/-}$ and IL-22$^{-/-}$ mice were bred and maintained under specific pathogen-free conditions in accredited animal facilities at the University of Edinburgh. Mice were aged >8 weeks old at the beginning of use and sex-matched. Both male and female mice were used in experiments. Mice were analyzed individually and no mice were excluded from the analysis, with the exception of exclusions due to technical errors in preparation of intestinal LPLs and failure of induction of Cre recombination by tamoxifen. All experiments were conducted in accordance with the UK Scientific Procedures Act of 1986 and had local ethical approval.

Treatment with small compounds, antibiotics, antibodies and rIL-22.

When indicated, mice were treated with indomethacin (5 mg/kg body weight/d, Sigma) or vehicle control (0.5% EtOH) in drinking water for 4-6 consecutive days for WT C57BL/6, *Rag1*$^{-/-}$ and IL-22$^{-/-}$ mice. In some experiments, mice were co-treated by intraperitoneal (i.p.) injection with an EP2 selective agonist (butaprost, Cayman) or an EP4 selective agonist (L-902,688, Cayman) at the dose of 10 μg per injection (one injection daily for 5 consecutive days) together with indomethacin from the starting day.

0.5% EtOH in PBS was used as vehicle control. As indicated, mice were treated with an EP4 selective antagonist (L-161,982 from Abcam, 10 mg/kg body weight/d) or vehicle control (0.5% DMSO) in drinking water for 6 consecutive days or through i.p. injection (20 μg per injection, one injection daily; vehicle control, 2% DMSO in PBS) for 5 consecutive days. To deplete ILCs, an anti-CD90.2 antibody (clone 30H12, BioXcell) or a rat IgG2b isotype control antibody (BioXcell) was injected i.p. into *Rag1*$^{-/-}$ mice at the dose of 250 μg per mouse every 3 days. Depletion efficiency was confirmed by flow cytometry. Recombinant IL-22 (PeproTech) was intravenously (i.v.) injected into *Rag1*$^{-/-}$ mice at the dose of 500 ng per mouse (one injection daily for 4 consecutive days) from the beginning of experiments. Control mice were injected i.v. with PBS. For antibiotic therapy, a cocktail of antibiotics containing ampicillin (0.5 mg/ml), gentamycin (0.5 mg/ml), metronidazole (0.5 mg/ml), neomycin (0.5 mg/ml), vancomycin (0.5 mg/ml) plus sucralose (4 mg/ml) was used as referenced to a previous report *(19)*. All antibiotics were purchased from Sigma and were administrated in drinking water together with indomethacin or vehicle for 5 d. When indicated, WT C57BL/6 mice were injected i.p. with lipopolysaccharides (LPS, Escherichia coli 0127:B8, Sigma) at a dose of 10 μg per mouse on d 5. Blood was withdrawn at 2 h after LPS injection or at the time that mice were culled. Serum was isolated following whole blood centrifugation and stored at -80^{o}C for analysis. In some experiments, mice were sacrificed 24 h after LPS/PBS injection and the peritoneal cavity lavaged (3 x 2 ml cold PBS) for neutrophil counts and lavage supernatant cytokines measurements. Other tissues such as spleen, liver, small and large intestines were then removed for further analysis.

Tamoxifen-induced EP4 deletion.

Induction of Cre recombination in CD90.2^{Cre}EP4$^{fl/+}$ mice by tamoxifen was described in a previous report *(25)*. Briefly, Tamoxifen (Sigma) was dissolved in sunflower oil/ethanol (10:1 ratio) at 10 mg/ml and injected i.p. into CD90.2^{Cre}EP4$^{fl/+}$ and control mice at the dose of 0.18 mg/g body weight/day for 3-5 consecutive days for Fig. 4B. Mice were injected i.p. with LPS (10 ug per injection per mouse) at 5 days after the last tamoxifen injection and blood was withdraw at 1.5 h after LPS injection. Splenic CD90.2^{+} cells were isolated using EasySep^{TM} Mouse CD90.2 Positive Selection Kit II (Stemcell technologies) and *Ptger4* gene expression was measured by real-time PCR in isolated splenic CD90.2^{+} cells to confirm the efficiency of conditional EP4 deletion. In Fig. S9C, tamoxifen was dissolved in sunflower oil excluding ethanol. Mice received tamoxifen by gavage at a dose of 0.18 mg/g body weight/day for five doses over seven days and were rested for further 4 days after the last tamoxifen treatment before being subjected to analysis.

DSS colitis.

WT C57BL/6 mice (8-9 weeks old at the beginning of experiments) were administrated with 2% (w/v) of dextran sulfate sodium (DSS, MW 36-50kDa, MP Biochemical) together with indomethacin (5 mg/kg body weight/d) or vehicle control (0.5% EtOH) in drinking water for 6 consecutive days. Recombinant IL-22 or PBS was injected i.p. into indicated mice at the dose of 500-1,000 ng per injection (one injection daily for 6 consecutive days) from the beginning of the experiments. Throughout the experimental timeline, mice were weighed and scored daily for a disease activity index (DAI) score to

allow for monitoring colitis progression and pathology. The DAI was scored by the following system *(37)*. Body weight: 0 (no or <1% weight loss compared to d 0 body weight), 1 (1-5% weight loss), 2 (5-10% weight loss), 3 (10-20% weight loss), and 4 (>20% weight loss); bleeding: 0 (no bleeding), 1 (blood present in/on faeces), 2 (visible blood in rectum), and 4 (visible blood on fur); and stool consistency: 0 (well formed/normal stool), 1 (pasty/semi-formed stool), 2 (pasty stool with some blood), 3 (diarrhea that does not adhere to anus), and 4 (diarrhea that does adhere to anus). Mice were immediately culled when body weight loss was greater that 25% or the total colitis score was 9 or higher.

Liver histology.

Liver samples were fixed with 10% neutral buffered formalin solution (Sigma), embedded in paraffin, and 5 μm sections were used for staining with hematoxylin and eosin (H&E). Adjustment of white balance was applied to the entire images.

Bacteria culture.

Counts of gut bacterial translocation to the liver were performed as described in a previous report *(19)*. Briefly, livers were removed under aseptic conditions and mechanically homogenized in sterile PBS. Tissue homogenates were serially diluted and cultured on LB agar (Sigma) at 37^{o}C for 2 days for subsequent colony counts.

Isolation of intestinal lamina propria cells.

Intestinal lamina propria (LP) cells were isolated as described previously *(38)*. In brief, mice were culled and their intestines removed and placed in cold PBS. After removing any remaining fatty and mesenteric tissues, samples were cut open longitudinally and any contents removed before being washed with HBSS buffer containing 2% FCS, and then cut into 0.5 cm pieces. Intestines were shaken at 37^{o}C for 15 min in HBSS containing 2 mM EDTA. After washing with pre-warmed HBSS buffer, intestines were again shaken at 37^{o}C for 30 min in HBSS containing 2 mM EDTA followed by wash with HBSS. Intestines were then transferred into gentleMACS C tubes (Miltenyi) digested in RPMI 1640 medium containing 10% FCS, 1% L-glutamine and antibiotics with 1.25 mg/ml collagenase IV (Roche) and 30 ug/ml DNase-I (Roche) by shaking at 37^{o}C for 30 min. Digested tissues were homogenized by gentleMACS disassociator running the programme m_intestine_01 and mashed through 40 μm cell strainer and flushed through HBSS containing 2% FCS. After centrifugation, cells were resuspended in complete RPMI 1640 medium for counting, staining, culture and/or sorting.

***In vitro* cell culture.**

MACS sorted small intestinal LP CD45^{+} cells, FACS sorted intestinal LP CD45^{+}Lin^{-} CD90.2^{+}KLRG1^{-}CCR6^{+} ILC3s, total *Rag1*$^{-/-}$ spleen cells, or FACS sorted splenic/bone marrow CD3^{-}CD11b^{-}CD11c^{-}CD4^{+} ILCs were cultured in completed RPMI 1640 medium (Gibco) supplemented with 10% FBS, 2-Mercaptoethanol (50 μM, Gibco), L-glutamine (2 mM, Gibco) and antibiotics (Penicillin and Streptomycin, 100 U/ml, Gibco). When indicated, recombinant IL-23 (20 ng/ml, eBioscience), IL-1β (20 ng/ml), IL-2 (10 ng/ml), IL-7 (10 ng/ml), indomethacin (10 μM, Sigma), PGE_2 (10 μM for detection of pCREB

and 100 nM for all other experiments except dose-response experiments, Cayman), an EP2 agonist butaprost (500 nM, Cayman), an EP4 agonist CAY10598 (500 nM, Cayman), an EP2 antagonist PF-04418948 (10 μM, Cayman), an EP4 antagonist L-161,982 (10 μM, Cayman), db-cAMP (300 μM, Sigma), 3-isobutyl-1-methylxanthine (IBMX, 500 μM for spleen cells and 100 μM for gut LPLs, Cayman), H-89 (10 μM, Merck), STAT3 inhibitor VI (S31-201, 25 μM, Merck), RORγt inhibitor (SR2211, 10 μM, Cayman), Ahr inhibitor (CH-223191, 10 μM, Merck) and their respective vehicle control (i.e. EtOH or DMSO) or combination of these reagents were added into cell cultures. For detecting cytokines in supernatants, cells were cultured for overnight or for 3 d as indicated in figure legends, and for intracellular staining of IL-22, cells were stimulated with IL-23 for 3-4 h in the presence of 0.2% GolgiPlug (BD Bioscience). *In vitro* cell cultures were performed in triplicates and repeated two or more times.

FACS sorting.

For purifying ILC3s from the small intestine of *Rag1*$^{-/-}$ mice, CD45^{+} LP cells were first isolated by MACS using mouse CD45 Microbeads (Miltenyi) and then stained with anti-CD45 eFluor450 or APC-Cy7 (clone 30-F11, eBioscience), anti-CD11c PE (clone N418, BioLegend), anti-CD11b PE (clone M1/70, eBioscience), anti-NK1.1 PE (clone PK136, eBioscience), anti-CD90.2 FITC or PE-Cy7 (clone 53-2.1, eBioscience), anti-KLRG1 APC (clone 2F1, eBioscience), anti-CCR6 Brilliant Violet (clone 29-2L17, Biolegend) on ice for 30 min. Alive CD45^{+}Lin^{-}(CD11c^{-}CD11b^{-}NK1.1^{-})CD90.2^{+}KLRG1^{-}CCR6^{+} ILC3s were sorted by FACSAria II (BD Bioscience). For purifying ILC3s from bone marrow and spleens of WT C57BL/6 mice, the CD4^{+} cell population was first isolated by MACS

with mouse CD4 MicroBeads (Miltenyi) and then stained with anti-CD3e PE (clone 145-2C11, eBioscience), anti-CD11b FITC (clone M1/70, BioLegend) and anti-CD4 PerCP-Cyanine5.5 (clone RM4-5, eBioscience) on ice for 30 min. In some experiments, an anti-CD11c PE (clone N418, BioLegend) was also used. Alive Lin^-($CD3^-CD11b^-CD11c^-$)$CD4^+$ cells were sorted by FACSAria II (BD Bioscience).

Surface and intracellular staining.

For surface staining, cells were first stained with the Fixable Viability Dye eFluor® 780 (eBioscience) on ice for 30 min to exclude dead cells. After wash, cells were stained on ice for another 30 min with indicated Abs such as anti-CD45 eFlour® 450, anti-CD3e PE, anti-CD11c PE, anti-CD11b PE, anti-B220 PE (clone RA3-6B2, eBioscience), anti-CD90.2 FITC, anti-CD4 PerCP-Cyanine5.5 or APC. Staining with Annexin V was performed using the FITC-Annexin V staining kit (Biolegend). For intracellular staining of IL-22, cells were stimulated with IL-23 (20 ng/ml) for 3-4 h in the presence of GolgiPlug (BD Bioscience). After staining with the Fixable Viability Dye eFluor® 780 and surface markers, cells were fixed by the BD Cytofix/Cytoperm Fixation buffer (BD Bioscience) for 30 min and then stained with anti-human/mouse IL-22 APC (clone IL22JOP, eBioscience) in the BD Perm/Wash Buffer on ice for 1 h. For staining of RORγt, a Foxp3/Transcription Factor Fix and Staining Buffer (eBioscience) and Anti-Mouse ROR-γt PerCP-eFluor710 (clone B2D, eBioscience) were used. For staining of peritoneal $CD11b^+$Ly-$6G^+$ neutrophils, peritoneal cells were first stained with Fixable Viability Dye eFluor® 780 on ice for 30 min. After wash, cells were stained on ice for another 30 min with anti-CD45 eFlour® 450, anti-CD11b FITC and anti-Ly-6G (Gr-1)

APC (clone RB6-8C5, eBioscience). To stain p-CREB, cells were stimulated with 10 uM of PGE_2 or vehicle at 37°C for 30 min, then fixed by a Foxp3/Transcription Factor Fix buffer (eBioscience) for overnight followed by staining with surface markers and a Phospho-CREB (Ser133) XP Rabbit mAb (clone D1G6, Cell Signaling) or a normal rabbit IgG for 1 h. After washing, cells were incubated with AF680 Donkey anti-Rabbit IgG for another 30 min. To stain pSTAT3, fresh spleen cells from *Rag1*$^{-/-}$ mice were cultured with PGE_2 or vehicle for 5 h and then stimulated with IL-23 for 15 min. Cells were fixed by the Foxp3/Transcription Factor Fix buffer for overnight followed by staining with surface markers and Alexa Fluor 488 Mouse Anti-STAT3(pS727) (clone 49, BD Bioscience). Flow cytometry was performed on the BD LSRFortessa (BD Bioscience) and analyzed by FlowJo software (Tree Star).

Enzyme-linked immunosorbent assay (ELISA).

For detection of cytokines in serum and supernatants of cell cultures or peritoneal lavage fluids, commercial ELISA kits were used according to the manufacturers' instructions. ELISA Ready-SET-Go!® kits for mouse IL-22 and IL-6 were obtained from eBioscience, while the Mouse TNF-α ELISA MAX™ Deluxe was purchased from BioLegend.

Gene expression and Real-time PCR.

RNA purification from sorted ILC3s or homogenized terminal ileum tissues was performed by using the Rneasy Mini Kit (Qiagen). cDNA was obtained by reverse transcription using the High-capacity cDNA Reverse Transcription Kits (ABI). Samples were analyzed by real-time PCR with SYBR Premix Ex Taq II (Tli RNase H Plus) kit

(Takara) or GoTaq qPCR Master Mix (Promega) on the Applied Biosystem 7900HT Fast machine. Below primers (some were obtained from ref. *39-47*) were used**.** *Il22* forward, 5'-CATGCAGGAGGTGGTACCTT-3'; *Il22* reverse, 5'-CAGACGCAAGCATTT CTCAG-3'. *Il22ra1* forward, 5'-TGCTCTGTTATCTGGG CTACAA-3'; *Il22ra1* reverse, 5'-TCAGGACACGTTGGACGTT-3'. *Il10rb* forward, 5'-TCTCTTCCACAGCACCT GAA-3'; *Il10rb* reverse, 5'-GAACACCTCGGCCTCCTC-3'. *Reg3b* forward, 5'-TGGGAATGGAGTAAAATG-3'; *Reg3b* reverse, 5'-GGCAACTTCACCTCACAT-3'. *Reg3g* forward, 5'-CCATCTTCACGTAGCAGC-3'; *Reg3g* reverse, 5'-CAAGATGTCCT GAGGGC-3'. *Muc1* forward, 5'-GGTTGCTTTGGCTATCGTCTATTT-3'; *Muc1* reverse, 5'-AAAGATGTCCAGCTGCCCATA-3'. *Muc3* forward, 5'-CGTGGTCAACT GCGAGAATGG-3'; *Muc3* reverse, 5'-CGGCTCTATCTCTACGCTCTCC-3'. *Fut2* forward, 5'-TGTGACTTCCACCATCATCC-3'; *Fut2* reverse, 5'-TCTGACAGGGTTT GGAGCTT-3'. *Cldn1* forward, 5'-GAGGGACTGTGGATGTCCTG-3'; *Cldn1* reverse, 5'-ATGCCAATTACCATCAAGGC-3'. *Cldn2* forward, 5'-TGAACACGGACCACTGA AAG-3'; *Cldn2* reverse, 5'-TTAGCAGGAA GCTGGGTCAG-3'. *Ocln* forward, 5'-CATAGTCAGATGGGGGTGGA-3'; *Ocln* reverse, 5'-ATTTATGATGAACAGCCCCC-3'. *F11r* forward, 5'-CTGATCTTTGACCCCGTGAC-3'; *F11r* reverse, 5'-ACCAGACG CCAAAAATCAAG-3'. *Tjp1* forward, 5'-ACTCCCACTTC CCCAAAAAC-3'; *Tjp1* reverse, 5'-CCACAGCTGAAGGACTCACA-3'. *Tjp2* forward, 5'-CGGATTCCAGAC AAGGTGTT-3'; *Tjp2* reverse, 5'-ATTCACGTTGATTGTGGCTG-3'. *Tnfsf11* forward, 5'-CGCTTCCCGATGTTTCATG-3'; *Tnfsf11* reverse, 5'-GGTTAACCAAGATGG CTTCTATTACC-3'. *Tnfsf4* forward, 5'-GGGAAGGGGTTCAACCCCTGG-3'; *Tnfsf4* reverse, 5'-GAAGAGAGTTGCAGGCAGACA-3'. *Il17a* forward, 5'-TGTGAAGGTC

AACCTCAAAGTC-3'; *Il17a* reverse, 5'-GAGGGATATCTATCAGGGTCTTCA-3'. *Il23r* forward, 5'-CCAAGTATATTGTGCATGTGAAGA-3', *Il23r* reverse, 5'-AGCTT GAGGCAAGATATTGTTGT-3'. *Il1r1* forward, 5'-TGGAACAGAGCCAGTGTCAG-3'; *Il1r1* reverse, 5'-CAGGAGAAGTCGCAGGAAGT-3'. *Lta* forward, 5'-GTACCCAA CAAGGTGAGCAGC-3'; *Lta* reverse, 5'-CCAGGACAGCCCATCCACT-3'. Ltb forward, 5'-ACGCTTCTTCTTGGCTCGC-3'; Ltb reverse, 5'-ACCTCATAGGCGCTT GGATG-3'. *Il7ra* forward, 5'-GGAACAACTATGTAAGAAGCCAAAAACG-3'; *Il7ra* reverse, 5'-AAGATCATTGGGCAGAAAACTTTCC-3'. *Ccr6* forward, 5'-CCTCACA TTCTTAGGACTGGAGC-3'; *Ccr6* reverse, 5'-GGCAATCAGAGCTCTCGGA-3'. *Csf2* forward, 5'-GCATGTAGAGGCCATCAAAGA-3'; *Csf2* reverse, 5'-CGGGTCTGCACA CATGTTA-3'. *Bcl2* forward, 5'-AGTACCTGAACCGGCATCTG-3'; *Bcl2* reverse, 5'-AGGTATGCACCCAGAGTGATG-3'. *Bcl2l1* forward, 5'-ATGACCACCTAGAGCC TTGGA-3'; *Bcl2l1* reverse, 5'-GAAGAGTGAGCCCAGCAGAAC-3'. *Ptger4* forward, 5'-CCTAACCCCACCCTACAGGT-3'; *Ptger4* reverse, AGAAGGACGCGTTGAC TCC-3'. *Gapdh* forward, 5'-TGAACGGGAAGCTCACTGG-3'; *Gapdh* reverse, 5'-TCCACCACCCTGTTGCTGTA-3'. Expression of genes *Rorc* (Mm01261022_m1), *Ahr* (Mm00478932_m1), *Stat3* (Mm01219775_m1), *Id2* (Mm00711781_m1), *Tcf7* (Mm00493445_m1), *Zbtb16* (Mm01176868_m1), *Tox* (Mm00455231_m1), *Nfil3* (Mm00600292_s1) were measured by Taqman Gene Expression Master Mix (Life Technologies) with respective primer sets obtained from Life Technologies. Expression was normalized to mouse glyceraldehyde-3-phosphate dehydrogenase (*Gapdh*) and presented as relative expression to control group by the $2^{-\Delta\Delta Ct}$ method.

Gene expression analysis of neonatal sepsis blood cells.

Gene transcription levels were measured by transcription microarray in a study by Smith *et al. (15)* on human neonates comparing confirmed bacterial infection (n=27 independent neonates) with non-infection controls (n=35 independent neonates). Processed and normalized data for genes *PTGES2* and *PTGER4* were retrieved from this study and probability density functions computed for each gene, per group. For each gene, the hypothesis of differential expression between infected and control neonates was tested through a Wilcoxon-Rank-Sum test. A separate hypothesis of different inter-subject variability was tested for through Fligner-Killeen tests. Data of blood neutrophil counts in neonatal sepsis and control patients were retrieved from our previous report *(15)* to complete a new analysis work for investigating their association with *PTGES2* and *PTGER4* gene expression by non-parametric Spearman correlation test.

Human ILC3 sort and culture and human IL-22 analysis.

Human $Lin^{-}CD161^{+}CD127^{+}CRTH2^{-}CD117^{+}$ ILC3s were sorted from peripheral blood of healthy donors. Lineage markers used for sorting included CD1a (clone HI149), CD3 (clone OKT3), CD14 (clone HCD14), CD34 (clone 581), CD94 (clone DX22), CD123 (clone 6H6), TCRα/β (clone IP26), TCRγ/δ (clone B1), BDCA2 (201A) and FcεR1 (clone AER-37). Anti-human CD161 (clone HP-3G10), CD127 (clone A019D5), CD117 (clone 104D2) and CD294/CRTH2 (clone BM16) were also used. All these Abs were obtained from Biolegend except CD294, which was purchased from BD Bioscience. Sorted human ILC3s were cultured with recombinant human IL-2 (5 ng/ml, Biolegend), human IL-23 (50 ng/ml, R&D system) and human IL-1β (50 ng/ml, Biolegend) for 4

days to induce IL-22 production. PGE_2 (100 nM) or vehicle was added into the culture system from the starting of culture. IL-22 levels in supernatants was measured by Human IL-22 ELISA MAX Deluxe (Biolegend).

Acute pancreatitis patients.

Human plasma samples were obtained with ethical approval and fully-informed consent (MREC ref. number 13/SS/0136, United Kingdom). Samples from our clinical archive obtained from persons presenting to hospital with acute pancreatitis (AP) over a three-month continuous period in 2013 (UKCRN ID: 16116) (http://public.ukcrn.org.uk/Search/StudyDetail.aspx?StudyID=16116) were included. The diagnosis of AP was made according to the Revised Atlanta Criteria 2012 *(48)*, namely an elevated serum amylase concentration > 300 IU/L in the context of abdominal pain, nausea and/or vomiting. Healthy volunteer blood samples were collected with ethical approval and fully-informed consent (REC ref. number 08/S1103/38, United Kingdom). Plasma aliquots were stored at -80^{o}C for <2 years with a single thaw before use. IL-22 concentrations were measured by ELISA as described above.

Statistical analysis.

All data were expressed as mean ± SEM. Statistical significance between two groups was examined by the Student's *t*-test or the Mann-Whitney test, while the one-way and two-way analysis of variance (ANOVA) with Bonferroni's, Holm-Sidak's or Newman-Keuls multiple comparisons test were used to evaluate multiple groups. Correlation analysis Fig. 3E and Fig. S13 was calculated by Pearson's correlation coefficient (r). Statistical

work was performed using Prism 6 software (GraphPad) and a *P* value of less than 0.05 was considered as significance.

Author Contributions

R.D., R.A.O., S.C., C.Yu, C.R., F.R. and C.Yao performed experiments. D.S., S.T., J.R., A.P., R.B.W., R.M.B., J.P.I., S.M.A., S.N. and R.M.M. provided technical expertise, essential reagents, transgenic mice and editorial advice. X.Z., C.S. and D.M. provided human plasma samples of AP patients and analyzed IL-22 levels. T.F. and P.G. performed work on neonatal sepsis and analysis of PG receptor expression on ILC3s. R.D., S.E.H., A.G.R. and C.Yao wrote the manuscript. S.E.H., A.G.R. and C.Yao conceived this project and supervised the research.

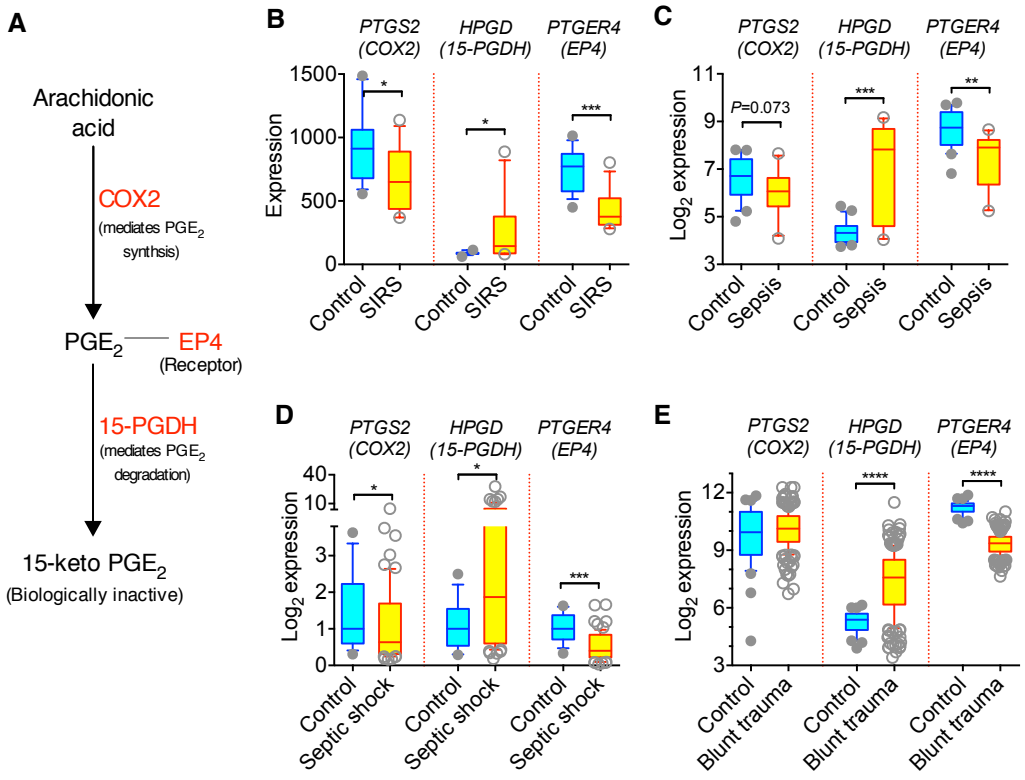

Fig. S1. Down-regulation of PGE_2-EP4 signaling is associated with development of severe systemic inflammatory diseases in humans. (A) A schematic chart indicates PGE_2 synthesis from arachidonic acid by COX2 (encoding by *PTGS2*) and degradation into biologically inactive 15-keto PGE_2 by 15-PGDH (encoding by *HPGD*). The PGE_2 receptor EP4 (encoding by *PTGER4*) is also shown. **(B)** Expression of *PTGS2*, *HPGD* and *PTGER4* in blood cells taken from patients diagnosed with systemic inflammatory response syndrome (SIRS, n=12) or healthy control individuals (n=18) on d 1. Data were retrieved from the Gene Expression Omnibus dataset GSE40012 *(49)*. **(C)** Expression of *PTGS2*, *HPGD* and *PTGER4* in blood cells taken from patients with sepsis (n=10) or healthy control (n=20). Data were retrieved from the Gene Expression Omnibus dataset GSE28750 *(50)*. **(D)** Expression of *PTGS2*, *HPGD* and *PTGER4* in blood cells taken from normal children (n=18) or children with septic shock (n=67) on d 1. Data were retrieved from the Gene Expression Omnibus dataset GSE13904 *(51)*. **(E)** Expression of *PTGS2*, *HPGD* and *PTGER4* in blood cells taken from healthy individuals (n=37) or patients with severe blunt trauma or burn injury (n=205) within 24 h from injury. Data were retrieved from the Gene Expression Omnibus dataset GSE36809 *(52)*. **P*<0.05, ***P*<0.01, ****P*<0.001, *****P*<0.0001 by 2-tailed Mann-Whitney test.

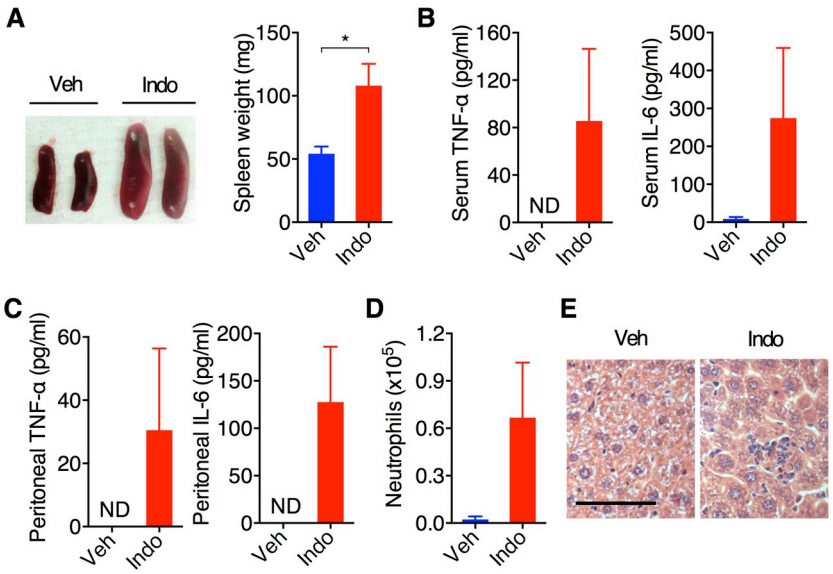

Fig. S2. Adaptive immune cells are not required for indomethacin-dependent systemic inflammation. *Rag1*$^{-/-}$ mice were treated with indomethacin (n=5) or vehicle control (n=4) in drinking water for 4 d. **(A)** Spleen size and weight. **(B)** IL-6 and TNF-α concentrations in serum. **(C)** IL-6 and TNF-α concentration in peritoneal cavity lavage fluids. **(D)** Accumulation of CD11b^{+}Ly-6G^{+} neutrophils in peritoneal cavities. **(E)** H&E staining histological sections of the liver. Data shown as mean ± SEM are pooled from two independent experiments. Scale bar, 50 μm. **P*<0.05 by the unpaired, 2-tailed student *t*-test. ND, not detected.

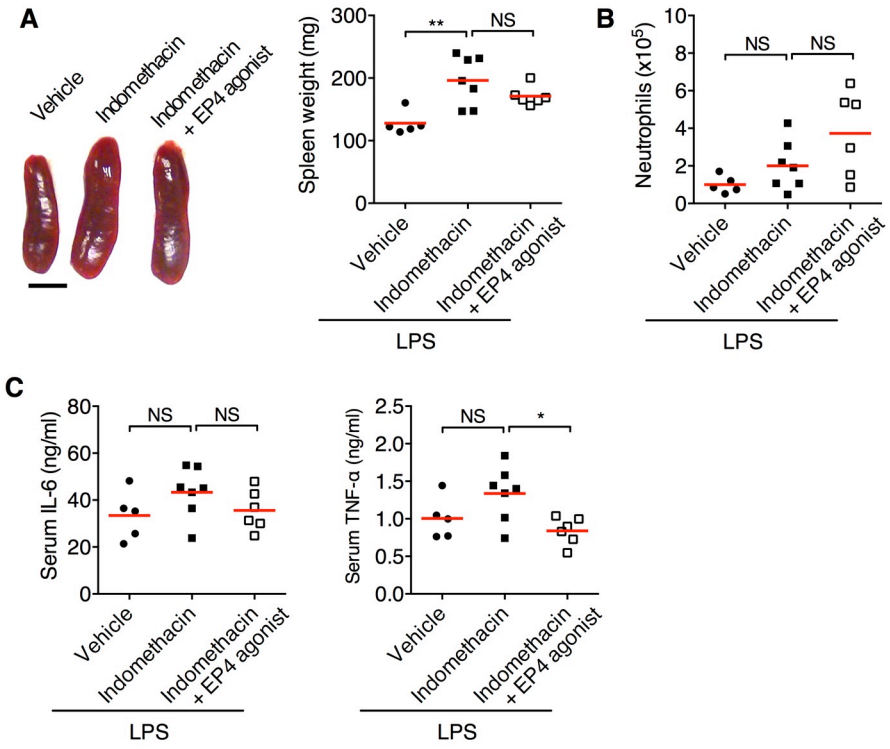

Fig. S3. IL-22 is required for control of systemic inflammation by PGE_2–EP4 signaling. Spleen size and weight (**A**), neutrophils in peritoneal cavity (**B**) and serum levels of TNF-α and IL-6 (**C**) of C57BL/6 IL-$22^{-/-}$ mice treated with indomethacin in drinking water plus administration (i.p.) of an EP4 agonist or vehicle control for 5 d followed by LPS challenge (i.p.) for another 24 h (A and B) or 2 h (C). Each point represents one mouse. Data are pooled from two independent experiments. Scale bar, 0.5 cm. **P*<0.05, ***P*<0.01 by one-way ANOVA. NS, not significant.

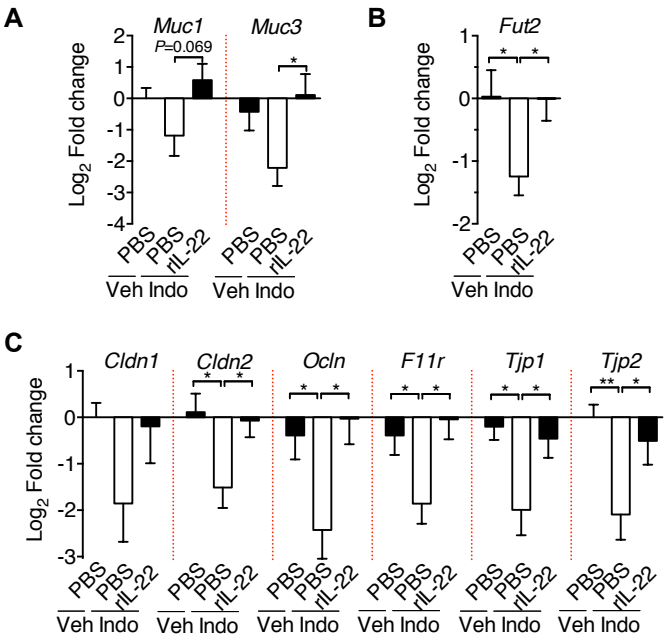

Fig. S4. Gene expression profile of intestinal barrier function. *Rag1*$^{-/-}$ mice treated with vehicle (n=9) or indomethacin in drinking water plus administration (i.v.) of rIL-22 (n=10) or PBS (n=10) for 5 d as in Fig. 3, C to G. **(A** to **C)** Gene expression of mucins (A), fucosylthransferase 2 (B) and tight junctions (C) in the terminal ileum. Expression was normalized to *Gapdh* gene and presented as relative expression (in Log_2 Fold Change) to the vehicle/PBS control group. Data shown as means ± SEM are pooled from three independent experiments. **P*<0.05, ***P*<0.01 by one-way ANOVA.

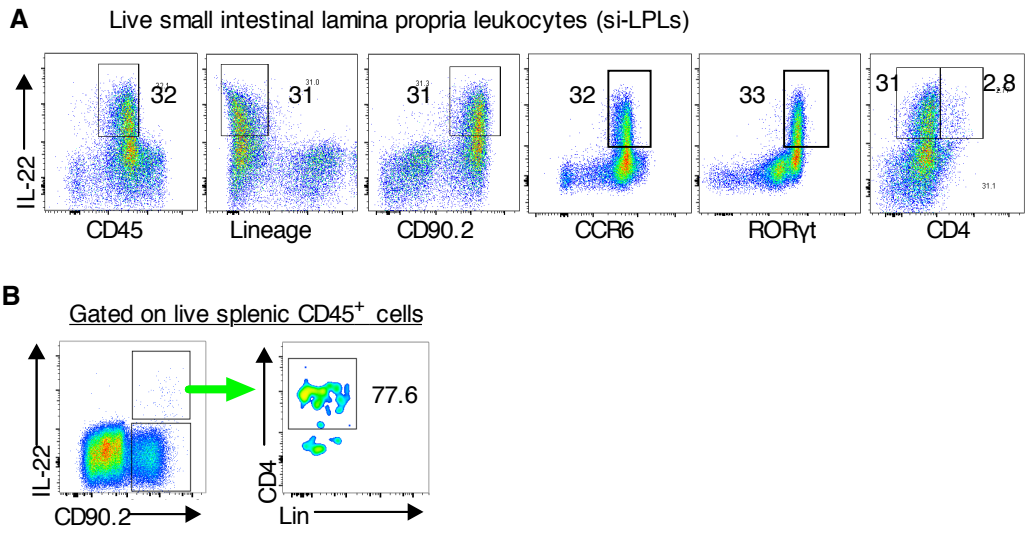

Fig. S5. Identification of IL-22-producing type 3 innate lymphoid cells in the gut and spleen. (A) Intracellular staining of small intestinal lamina propria lymphocytes (LPLs) from *Rag1*$^{-/-}$ mice cultured with IL-23 for 4 h. The result indicates that IL-22-expressing innate cells in the gut are CD45$^{+/Low}$Lineage^{-}(CD11c/CD11b/NK1.1)CD90.2^{+}CCR6^{+} RORγt^{+} ILC3s and most of these cells (>90%) do not express CD4. **(B)** Intracellular staining of total *Rag1*$^{-/-}$ spleen cells cultured with IL-23 for 4 h. The result indicates that all IL-22-expressing innate cells in the spleen are CD45^{+}Lin^{-}CD90.2^{+} and the majority (70-80%) of them are CD4^{+} ILC3s.

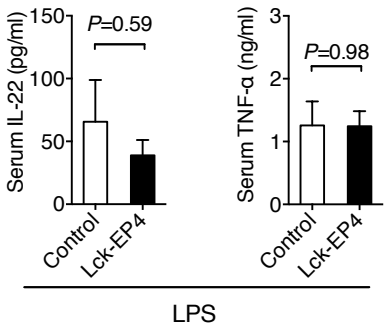

Fig. S6. PGE_2–EP4 signaling in T cells is not required for control of systemic inflammation. Serum levels of IL-22 and TNF-α of mice with specific EP4 deletion in T cells (i.e., Lck-EP4 mice mixed of $Lck^{Cre}EP4^{fl/+}$ and $Lck^{Cre}EP4^{fl/fl}$ mice, n=4) and control litter mates (mixed of Lck^{Cre}, $EP4^{fl/fl}$, $EP4^{fl/+}$ and $EP4^{+/+}$ mice, n=8) at 1.5 h after LPS challenge. Efficiency of EP4 deletion in T cells of $Lck^{Cre}EP4^{fl/+}$ (~50%) and $Lck^{Cre}EP4^{fl/fl}$ (~97%) mice comparing to control mice has been shown previously *(27)*. Data shown as means ± SEM are pooled from two independent experiments. *P* values are calculated by unpaired two-tailed Student's *t*-test.

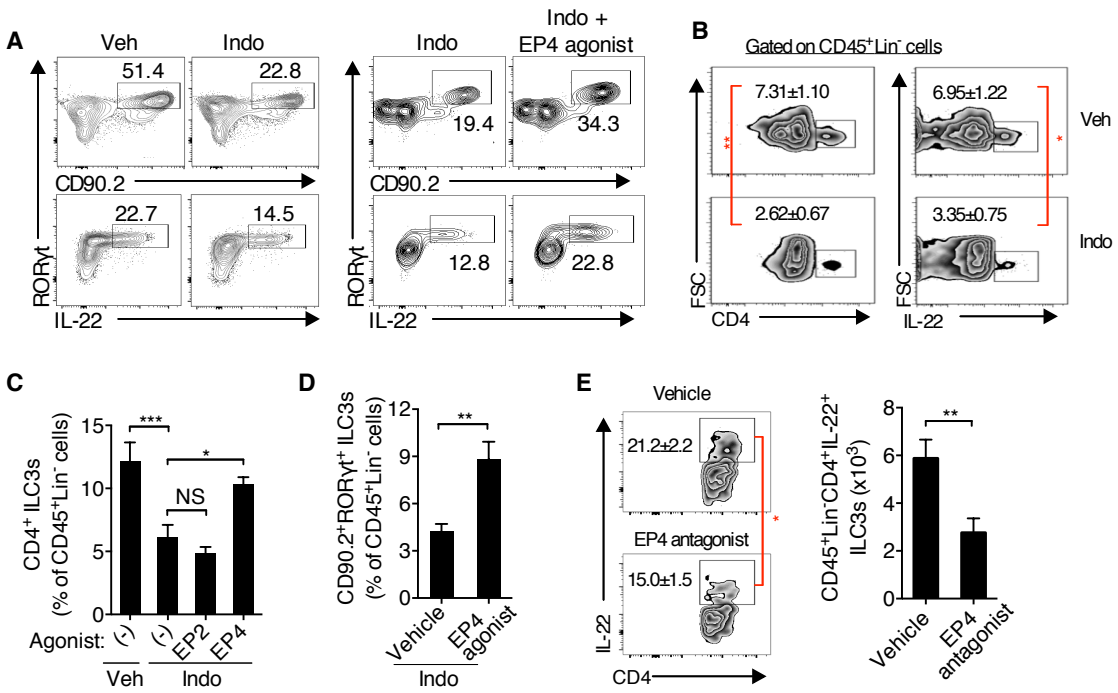

Fig. S7. PGE_2–EP4 signaling regulates innate lymphoid cell homeostasis in spleen. **(A)** Intracellular staining of small intestinal LPLs of C57BL/6 *Rag1*$^{-/-}$ mice treated with vehicle (n=9) or indomethacin in drinking water plus an EP4 agonist (n=8) or vehicle (n=10) for 4 days as in Fig.4C. Representative dot plot data show RORγt$^+$IL-22$^+$ cells within alive CD45$^+$ populations. **(B)** Frequencies of CD45$^+$Lin$^-$CD4$^+$ and CD45$^+$Lin$^-$IL-22$^+$ ILC3s in spleens of *Rag1*$^{-/-}$ mice treated with indomethacin (Indo, n=8) or vehicle (Veh, n=6) for 4 d. **(C)** Frequencies of CD45$^+$Lin$^-$CD4$^+$ ILC3s in spleen of *Rag1*$^{-/-}$ mice treated with vehicle (n=6) or indomethacin plus administration (i.p.) of agonist for EP2 (n=6), EP4 (n=6) or vehicle control (n=8) for 4 days. **(D)** Frequencies of CD45$^+$Lin$^-$ CD90.2$^+$RORγt$^+$ ILC3s in spleen of *Rag1*$^{-/-}$ mice treated with indomethacin plus administration (i.p.) of an EP4 agonist or vehicle control (n=8 per group) for 4 days. **(E)** Frequencies and numbers of CD45$^+$Lin$^-$CD4$^+$IL-22$^+$ ILC3s in spleens of *Rag1*$^{-/-}$ mice treated (i.p.) with an EP4 antagonist (n=10) or vehicle (n=9) for 4 d. Data shown as mean ± SEM are pooled from two independent experiments. **P*<0.05, ***P*<0.01, ****P*<0.001 by Mann-Whitney test (B, D and E) or one-way ANOVA (C).

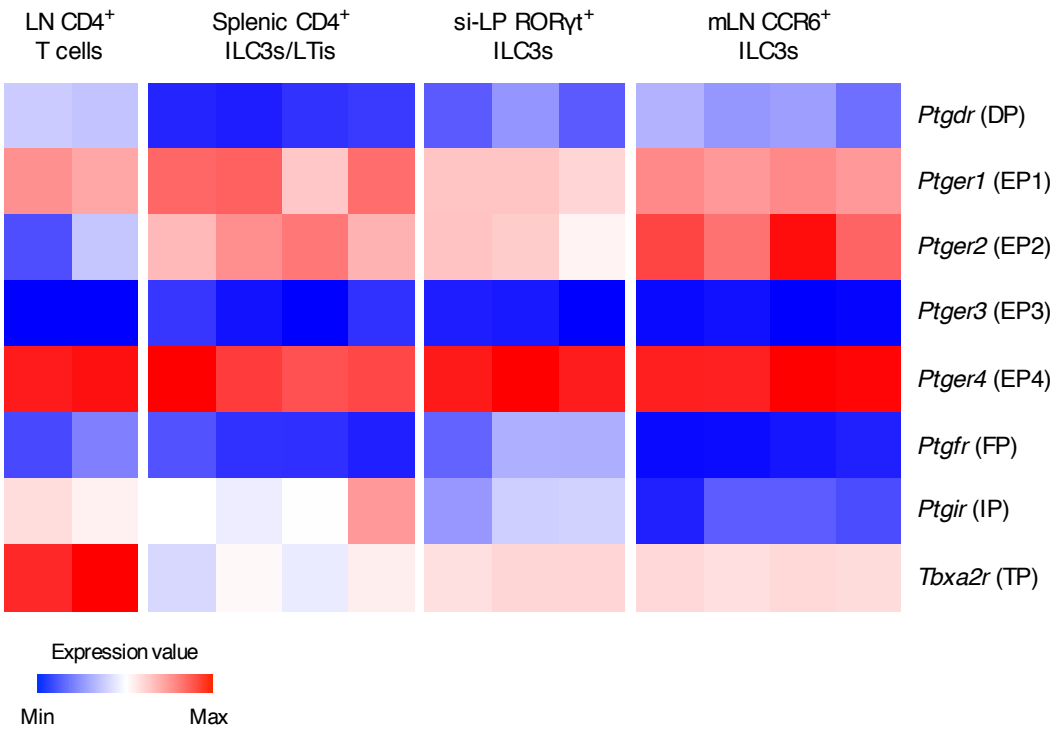

Fig. S8. Expression of PG receptors by ILC3s. Gene expression of PG receptors in FACS-sorted ILC3 populations isolated from various tissues including splenic Lin^- $CD90.2^+CD25^+CD4^+$ ILC3s/LTis (Lymphoid tissue inducer cells, n=4), small intestinal LP (si-LP) $CD45^+Lin^-NKp46^+ROR\gamma t^{hi}$ ILC3s (n=3), and mesenteric lymph node (mLN) $Lin^-CD90.2^+CD127^+CCR6^+ST2^-$ ILC3s (n=4). Gene expression in lymph node (LN) $TCR^+CD4^+CD8^-CD25^-CD62^{hi}CD44^{low}$ naïve T cells (n=2) was used as control. Results suggest that in ILC3s the PGE_2 receptor EP4 (encoded by *Ptger4*) is the most expressed among 8 subtypes of PG receptors. While ILC3s may also express PGE_2 receptors EP1 (encoded by *Ptger1*) and EP2 (encoded by *Ptger2*) and thromboxane A2 receptor TP (encoded by *Tbxa2r*), ILC3s are unlikely to express PGD_2 receptor DP (encoded by *Ptgdr*), PGE_2 receptor EP3 (encoded by *Ptger3*), $PGF_{2\alpha}$ receptor FP (encoded by *Ptgfr*) and PGI_2 receptor IP (encoded by *Ptgir*). Data were retrieved from the Gene Expression Omnibus dataset GSE37448 for LN $CD4^+$ T cells and si-LP $ROR\gamma t^+$ ILC3s *(53),* GSE46468 for splenic $CD4^+$ ILC3s/LTis *(54)*, and GSE67076 for mLN $CCR6^+$ ILC3s *(55)*.

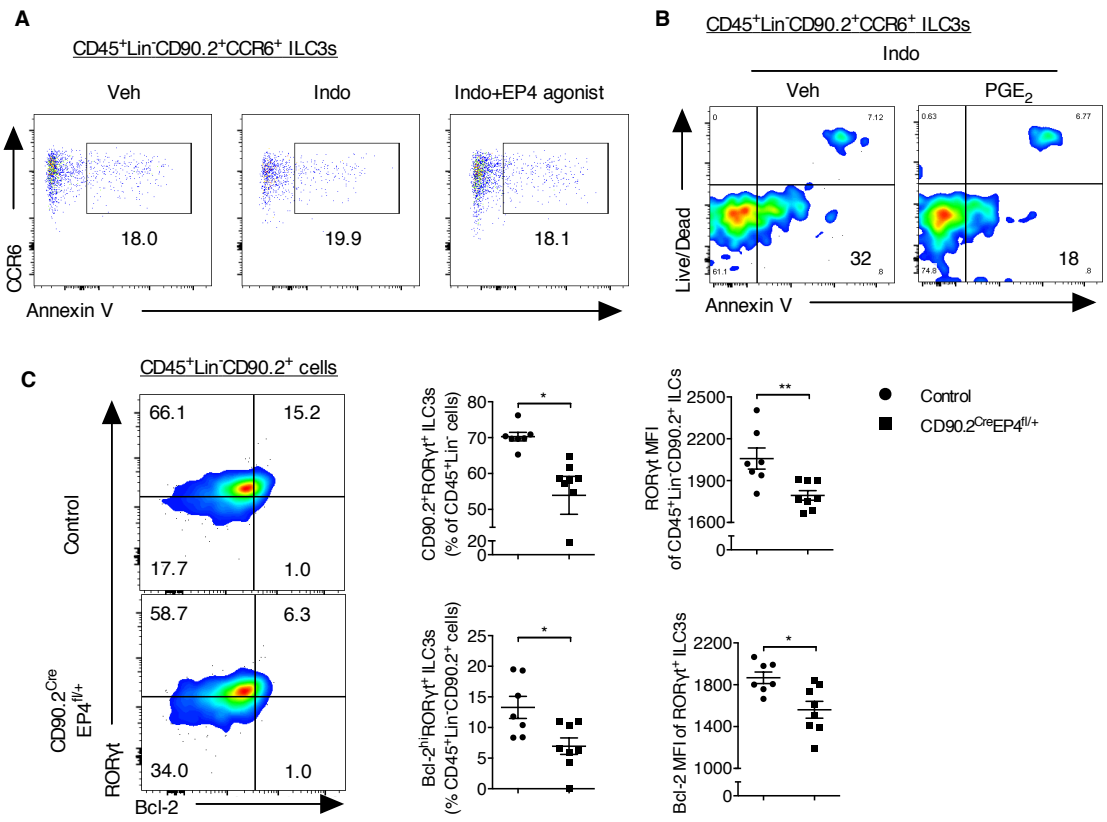

Fig. S9. PGE_2 prevents ILC3 apoptosis and augments IL-7 responsiveness *in vitro*. **(A)** Expression of Annexin V in $CD45^+Lin^-CD90.2^+CCR6^+$ ILC3s from mesenteric lymph nodes of C57BL/6 mice treated with vehicle (n=4) or indomethacin in drinking water plus an EP4 agonist (n=7) or vehicle (n=5) for 5 days. **(B)** Mesenteric lymph node cells of *Rag1*$^{-/-}$ mice were cultured *in vitro* with indomethacin in the presence or absence of PGE_2 for 24 h. Data showing expression of Annexin V in $CD45^+Lin^-CD90.2^+CCR6^+$ ILC3s are representative of two independent experiments. **(C)** Mesenteric lymph node cells from tamoxifen-treated $CD90.2^{Cre}EP4^{fl/+}$ (n=8) or control (n=7) mice were cultured *in vitro* with IL-7 for 24 h. Expression of Bcl-2 and RORγt in $CD45^+Lin^-CD90.2^+$ ILCs were shown. **P*<0.05, ***P*<0.01 by two-tailed unpaired Student's *t*-test.

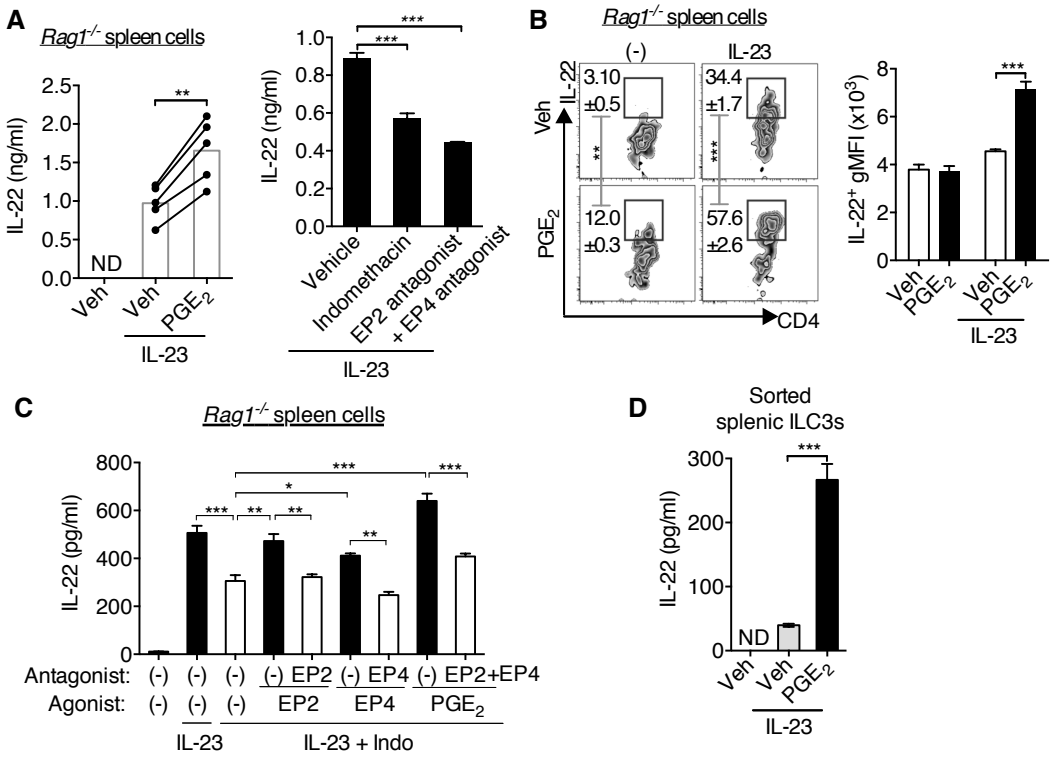

Fig. S10. PGE_2 promotes IL-22 production from splenic ILC3s via EP2 and EP4 receptors *in vitro*. (A) IL-22 levels in supernatants of total *Rag1*$^{-/-}$ spleen cells cultured with IL-23 and PGE_2, indomethacin or EP2 antagonist plus EP4 antagonist overnight. **(B)** Intracellular IL-22 expression in Lin$^-$(CD3$^-$B220$^-$Ter119$^-$CD11c$^-$)CD4$^+$ cells of *Rag1*$^{-/-}$ spleen cells cultured under indicated conditions for 4 h. **(C)** IL-22 levels in supernatants from total *Rag1*$^{-/-}$ spleen cells cultured with IL-23 without or with indomethacin plus agonists and/or antagonists for EP2 or EP4 as indicated overnight. **(D)** IL-22 production by Lin$^-$CD4$^+$ ILC3s sorted from spleen and/or bone marrow and then cultured with IL-23 in the presence or absence of PGE_2 for 3 d. Data shown as means ± SEM are representative of two (B-D) or three (A, right) or pooled from five (A, left) independent experiments. **P*<0.05, ***P*<0.01, ****P*<0.001 by one-way ANOVA (A right, B and C), unpaired (D) or paired (A left) Student's *t*-test or. ND, not detected.

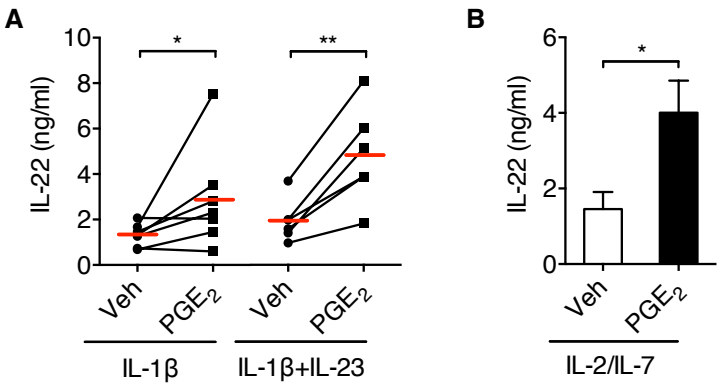

Fig. S11. Cytokine response of ILC3s regulated by PGE_2. IL-22 levels in supernatants of LPLs isolated from small intestines of *Rag1*$^{-/-}$ mice and then cultured with indicated cytokines in the presence or absence of PGE_2 overnight (A) or for 3 days (B). Data shown as means ± SEM are pooled from 2-3 independent experiments. For the panel A, n=6-7 biological replicates and for the panel B, n=4 biological replicates. **P*<0.05, ***P*<0.01 by 2-way ANOVA (A) or unpaired Student's *t*-test (B).

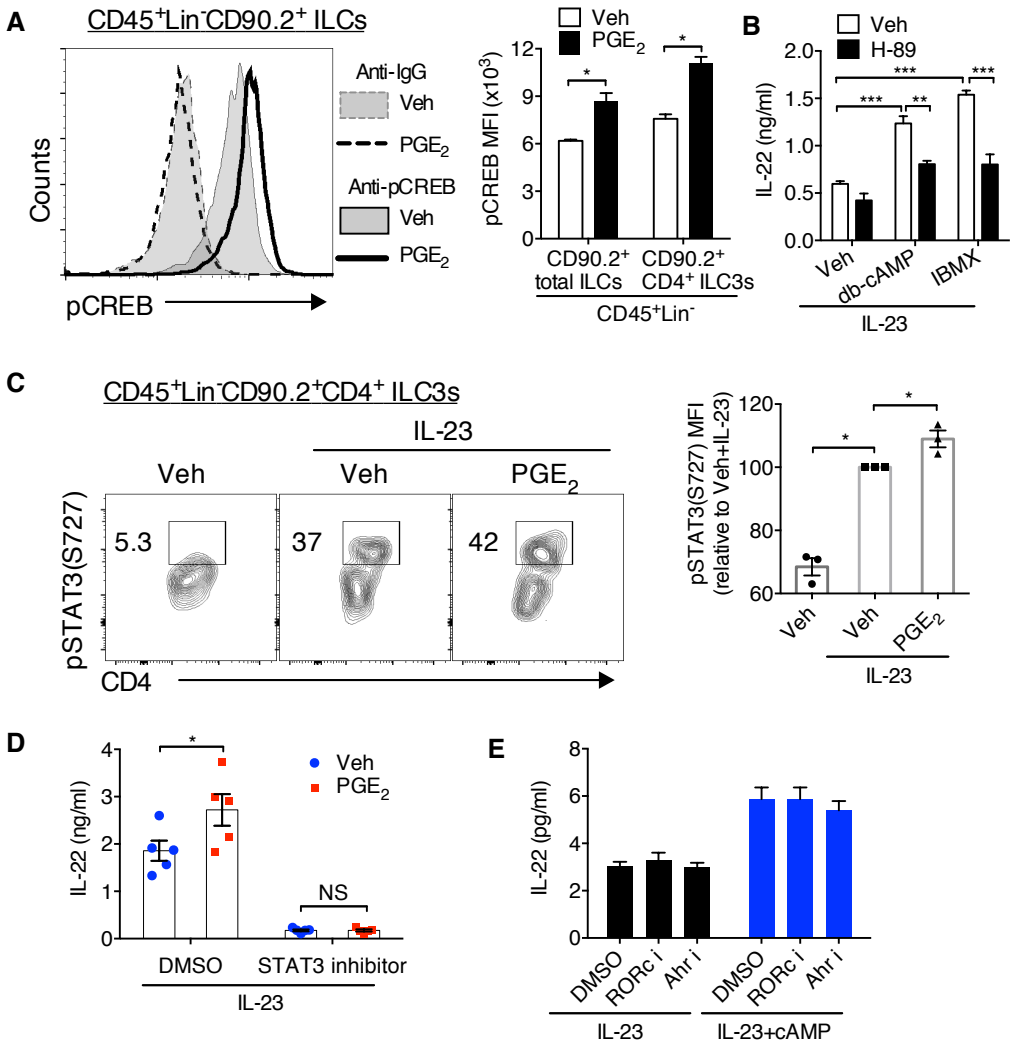

Fig. S12. Cyclic AMP-PKA and IL-23-STAT3 (transcription factor signal transducer and activator of transcription) signaling pathways mediate innate IL-22 production *in vitro*. **(A)** Intracellular expression of phosphorylated CREB (pCREB) in splenic $CD45^+Lin^-CD90.2^+$ ILCs and $CD45^+Lin^-CD90.2^+CD4^+$ ILC3s stimulated with PGE_2 or vehicle for 30 min. MFI, mean fluorescence intensity. Data shown as means ± SEM are representative of two independent experiments. **(B)** IL-22 production in supernatants from total *Rag1*$^{-/-}$ splenocytes cultured with IL-23 plus db-cAMP or IBMX with or without H-89 overnight. db-cAMP, dibutyryl-cAMP; IBMX, 3-isobutyl-1-methylxanthine. Data shown as means ± SEM are representative of two independent experiments. **(C)** Intracellular expression of phosphorylated STAT3 (pSTAT3) in splenic $CD45^+Lin^-CD90.2^+CD4^+$ ILC3s stimulated with PGE_2 or vehicle for 5 h and then restimulated with IL-23 for a further 15 min. Data shown as means ± SEM are pooled from three independent experiments. **(D)** IL-22 production in supernatants from small intestinal LPLs of *Rag1*$^{-/-}$ mice cultured with IL-23 with or without PGE_2 and a STAT3

inhibitor overnight. Data shown as means ± SEM (n=5 biological replicates). **(E)** IL-22 production in supernatants from total *Rag1*$^{-/-}$ splenocytes cultured with IL-23 with or without db-cAMP and RORγt inhibitor (RORc i) or Ahr inhibitor (Ahr i) overnight, suggesting that neither RORγt nor Ahr is likely needed for cAMP-enhanced IL-22 production. Data shown as means ± SEM are representative of four independent experiments. **P*<0.05, ***P*<0.01, ****P*<0.001 by one-way ANOVA.

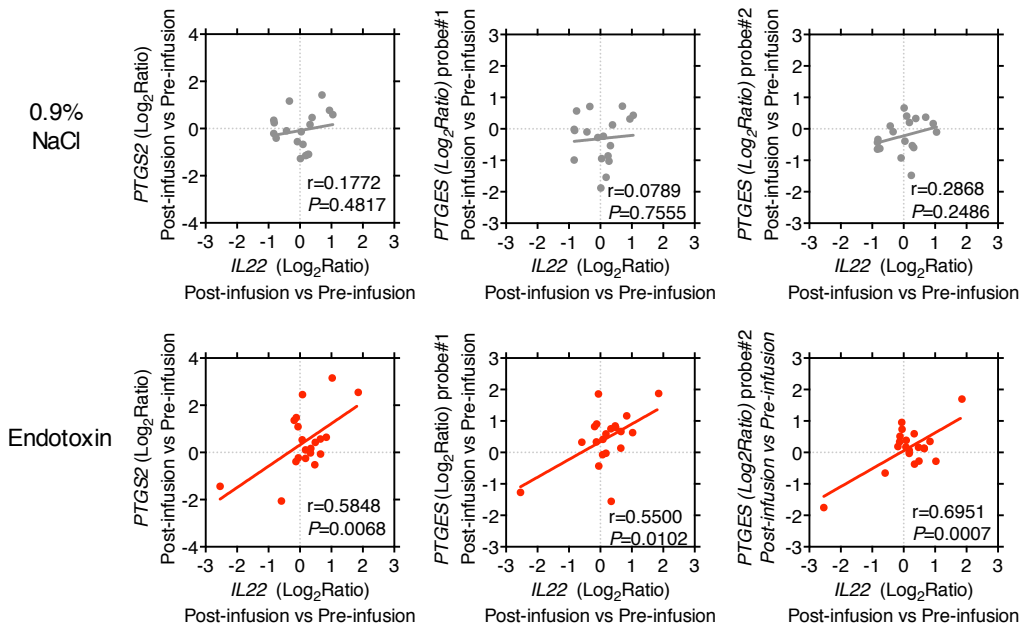

Fig. S13. Positive correlations between gene expression of *IL22* and PGE_2 synthases in response to endotoxin infusion in humans. Expression of *IL22* (encoding human IL-22), *PTGS2* (encoding human COX2) and *PTGES* (encoding human mPGES) genes in peripheral blood leukocytes obtained from healthy individuals before or after (2-24 h) infusion with endotoxin (CC-RE-Lot 2) or 0.9% sodium chloride ***(29)***. Raw data were retrieved from the Gene Expression Omnibus dataset GSE3284 ***(29)***. Data shown here were presented as the 'Log_2Ratio' of post-infusion (2, 4, 6, 9, 24 h) vs pre-infusion (0 h) of the endotoxin. Statistical analysis was calculated by the Pearson correlation coefficients (r).

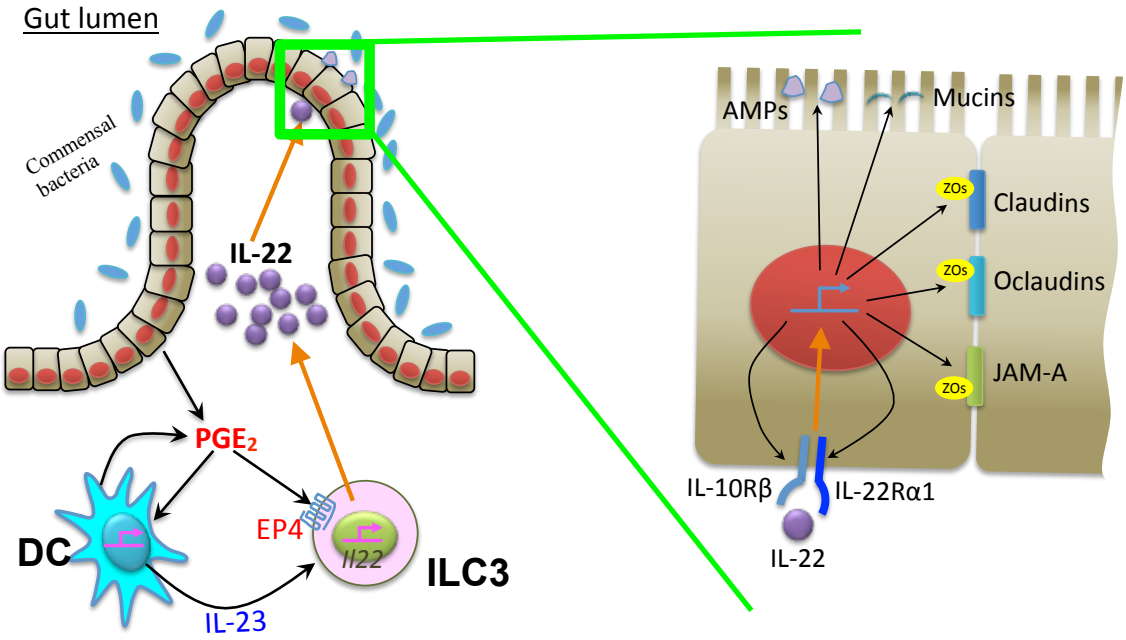

Fig. S14. A proposed model. PGE_2, produced by many types of cells such as macrophages, dendritic cells and gut epithelial cells, through the EP4 receptor contributes to maintaining ILC3 homeostasis. PGE_2 also works together with IL-23 to promote IL-22 production by ILC3s. The PGE_2/EP4/ILC3/IL-22 axis protects intestinal epithelial barrier function through amplification of IL-22-IL-22R signaling and promotion of production of antimicrobial peptides, mucus family proteins and tight junctions. This enables prevention of peripheral bacterial dissemination and subsequently contributes to control of systemic inflammation.

References

1. R.S. Hotchkiss, I.E. Karl, The pathophysiology and treatment of sepsis. *N. Engl. J. Med.* **3481,** 138-150 (2003).
2. S.P. LaRosa, S.M. Opal, Immune aspects of sepsis and hope for new therapeutics. *Curr. Infect. Dis. Rep.* **14,** 474-483 (2012).
3. J. Cohen, S. Opal, T. Calandra, Sepsis studies need new direction. *Lancet Infect. Dis.* **12,** 503-505 (2012).
4. T. Hirata, S. Narumiya, Prostanoids as regulators of innate and adaptive immunity. *Adv. Immunol.* **116,** 143-174 (2012).
5. E. Ricciotti, G.A. FitzGerald, Prostaglandins and inflammation. *Arterioscler. Thromb. Vasc. Biol.* **31,** 986-1000 (2011).
6. R.O. Day, Non-steroidal anti-inflammatory drugs (NSAIDs). *BMJ* **346,** f3195 (2013).
7. G.R. Bernard, *et al.,* The effects of ibuprofen on the physiology and survival of patients with sepsis. The ibuprofen study group. *N. Engl. J. Med.* **336,** 912-918 (1997).
8. M.T. Haupt, M.S. Jastremski, T.P. Clemmer, C.A. Metz, G.B. Goris, Effect of ibuprofen in patients with severe sepsis: a randomized, double-blind, multicenter study. The ibuprofen study group. *Crit. Care Med.* **19,** 1339-1347 (1991).
9. D.M. Aronoff, Cyclooxygenase inhibition in sepsis: is there life after death? *Mediat. Inflamm.* **2012,** 696897 (2012).
10. D.P. Eisen, Manifold beneficial effects of acetyl salicylic acid and non-steroidal anti-inflammatory drugs on sepsis. *Intensive Care Med.* **38,** 1249-1257 (2012).
11. D.L. Stevens, Could nonsteroidal anti-inflammatory drugs (NSAIDs) enhance the progression of bacterial infections to toxic shock syndrome? *Clin. Infect. Dis.* **21,** 977-980 (1995).
12. A. Legras, *et al.,* A multicentre case-control study of nonsteroidal anti-inflammatory drugs as a risk factor for severe sepsis and septic shock. *Crit. Care.* **13,** R43 (2009).
13. B.H. Lee, *et al.,* Association of body temperature and antipyretic treatments with mortality of critically ill patients with and without sepsis: multi-centered prospective observational study. *Crit. Care.* **16,** R33 (2012).

14. J.N. Fullerton, A.J. O'Brien, D.W. Gilroy, Lipid mediators in immune dysfunction after severe inflammation. *Trends. Immunol.* **35,** 12-21 (2014).
15. C.L. Smith, *et al.,* Identification of a human neonatal immune-metabolic network associated with bacterial infection. *Nat. Commun.* **5,** 4649 (2014).
16. M. Bruegel, *et al.,* Sepsis-associated changes of the arachidonic acid metabolism and their diagnostic potential in septic patients. *Crit. Care. Med.* **40,** 1478–1486 (2012).
17. K. Kabashima, *et al.,* The prostaglandin receptor EP4 suppresses colitis, mucosal damage and CD4 cell activation in the gut. *J. Clin. Invest.* **109,** 883–893 (2002).
18. T. Chinen, *et al.,* Prostaglandin E_2 and SOCS1 have a role in intestinal immune tolerance. *Nat. Commun.* **2,** 190 (2011).
19. G.F. Sonnenberg, *et al.,* Innate lymphoid cells promote anatomical containment of lymphoid-resident commensal bacteria. *Science* **336,** 1321-1325 (2012).
20. R., Sabat, W. Ouyang, K. Wolk, Therapeutic opportunities of the IL-22-IL-22R1 system. *Nat. Rev. Drug. Discov.* **13,** 21-38 (2014).
21. G.F., Sonnenberg, L.A. Fouser, D. Artis, Border patrol: regulation of immunity, inflammation and tissue homeostasis at barrier surfaces by IL-22. *Nat. Immunol.* **12,** 383-390 (2011).
22. G. Eberl, M. Colonna, J.P. Di Santo, A.N. McKenzie, Innate lymphoid cells: A new paradigm in immunology. *Science* **348,** aaa6566 (2015).
23. K. Kreymborg, *et al.,* IL-22 is expressed by Th17 cells in an IL-23-dependent fashion, but not required for the development of autoimmune encephalomyelitis. *J. Immunol.* **179,** 8098–8104 (2007).
24. Y. Goto, *et al.,* Innate lymphoid cells regulate intestinal epithelial cell glycosylation. *Science* **345,** 1254009 (2014).
25. B. Zonta, *et al.,* A critical Role for Neurofascin in regulating action potential Initiation through maintenance of the Axon Initial Segment. *Neuron* **69,** 945-956 (2011).
26. A. Schneider, *et al.,* Generation of a conditional allele of the mouse prostaglandin EP4 receptor. *Genesis* **40,** 7-14 (2004).
27. C. Yao, *et al.,* Prostaglandin E_2 promotes Th1 differentiation via synergistic amplification of IL-12 signalling by cAMP and PI3-kinase. *Nat. Commun.* **4**, 1685

(2013).

28. X. Guo, *et al.,* Induction of innate lymphoid cell-derived interleukin-22 by the transcription factor STAT3 mediates protection against intestinal infection. *Immunity* **40,** 25-39 (2014).
29. S.E. Calvano, *et al.,* A network-based analysis of systemic inflammation in humans. *Nature* **437,** 1032-1037 (2005).
30. J.E. Fishman, *et al.* The intestinal mucus layer is a critical component of the gut barrier that is damaged during acute pancreatitis. *Shock* **42,** 264-270 (2014).
31. D. Feng, *et al.* Interleukin-22 ameliorates cerulein-induced pancreatitis in mice by inhibiting the autophagic pathway. *Int. J. Biol. Sci.* **8,** 249-257 (2012).
32. B. Xiang, *et al*., Platelets protect from septic shock by inhibiting macrophage-dependent inflammation via the cyclooxygenase 1 signalling pathway. *Nat. Commun.* **4**, 2657 (2013).
33. L.E. Fredenburgh, *et al.,* Cyclooxygenase-2 deficiency leads to intestinal barrier dysfunction and increased mortality during polymicrobial sepsis. *J. Immunol.* **187,** 5255-5267 (2011).
34. S.M. Hamilton, C.R. Bayer, D.L. Stevens, A.E. Bryant, Effects of selective and nonselective nonsteroidal anti-inflammatory drugs on antibiotic efficacy of experimental group A streptococcal myonecrosis. *J. Infect. Dis.* **209,** 1429-1435 (2014).
35. Y. Zhang, *et al.,* Inhibition of the prostaglandin-degrading enzyme 15-PGDH potentiates tissue regeneration. *Science* **348**, aaa2340 (2015).
36. K. Németh, *et al.,* Bone marrow stromal cells attenuate sepsis via prostaglandin E_2-dependent reprogramming of host macrophages to increase their interleukin-10 production. *Nat. Med.* **15,** 42-49 (2009).
37. H.S. Cooper, S.N. Murthy, R.S. Shah, Sedergran, D. J. Clinicopathologic study of dextran sulfate sodium experimental murine colitis. *Lab. Invest.* **69**, 238-249 (1993).
38. C.C. Bain, A.M. Mowat. CD200 receptor and macrophage function in the intestine. *Immunobiology* **217,** 643-651 (2012).
39. Y. Chung, *et al.* Expression and regulation of IL-22 in the IL-17-producing CD4+ T lymphocytes. *Cell Res.* **16,** 902-907 (2006).

40. J.U. Johansson, *et al.* Suppression of inflammation with conditional deletion of the prostaglandin E2 EP2 receptor in macrophages and brain microglia. *J. Neurosci.* **33,** 16016-16032 (2013).
41. S. Buonocore, *et al.* Innate lymphoid cells drive interleukin-23-dependent innate intestinal pathology. *Nature* **464,** 1371-1375 (2010).
42. S. Jenkins, *et al.* Dendritic cell expression of OX40L ligand acts as a costimulatory, not polarizing, signal for optimal Th2 priming and memory induction in vivo. *J. Immunol.* **179,** 3515-3523 (2007).
43. J.H. Ju, *et al.* IL-23 induces receptor activator of NF-kB ligand expression on CD4+ T cells and promotes osteoclastogenesis in an autoimmune arthritis model. *J. Immunol.* **181,** 1507-1518 (2008).
44. L. Ma, *et al.* Association of brain immune genes with social behavior of inbred mouse strains. *J. Neuroinflammation* **12,** 75 (2015).
45. N. Burger-van Paassen, *et al.* Mucin Muc2 Deficiency and Weaning Influences the Expression of the Innate Defense Genes Reg3β, Reg3γ and Angiogenin-4. *PLoS ONE* **7,** e38798 (2012).
46. I. Hwang, *et al.* Tissue-specific expression of occluding, zona occludens-1, and junction adhesion molecule A in the duodenum, ileum, colon, kidney, liver, lung, brain, and skeletal muscle of C57BL/6 mice. *J. Physiol. Pharmacol.* **64,** 11-18 (2013).
47. C. Liu, *et al.* Gastric de novo Muc13 expression and spasmolytic polypeptide-expressing metaplasia during Helicobacter heilmannii infection. *Infect. Immun.* **82,** 3227-3239 (2014).
48. P.A. Banks*, et al.* Classification of acute pancreatitis—2012: revision of the Atlanta classification and definitions by international consensus. *Gut* **62,** 102-111 (2013).
49. G.P. Parnell, *et al.,* A distinct influenza infection signature in the blood transcriptome of patients with severe community-acquired pneumonia. *Crit. Care.* **16,** R157 (2012).
50. A. Sutherland, *et al.,* Development and validation of a novel molecular biomarker diagnostic test for the early detection of sepsis. *Crit. Care.* **15,** R149 (2011).
51. H.R. Wong, *et al.,* Genomic expression profiling across the pediatric systemic

inflammatory response syndrome, sepsis, and septic shock spectrum. *Crit. Care. Med.* **37,** 1558-1566 (2009).

52. W. Xiao, *et al.,* A genomic storm in critically injured humans. *J. Exp. Med.* **208,** 2581-2590 (2011).
53. M.L. Robinette, *et al.* Transcriptional programs define molecular characteristics of innate lymphoid cell classes and subsets. *Nat. Immunol.* **16,** 306–317 (2015).
54. L.A. Monticelli, G.F. Sonnenberg, M.C. Abt, T. Alenghat, *et al.* Innate lymphoid cells promote lung-tissue homeostasis after infection with influenza virus. *Nat. Immunol.* **12,** 1045-1054 (2011).
55. M.R. Hepworth, T.C. Fung, S.H. Masur, J.R. Kelsen, *et al.* Group 3 innate lymphoid cells mediate intestinal selection of commensal bacteria-specific CD4+ T cells. *Science* **348,** 1031-1035 (2015).

Figure 1

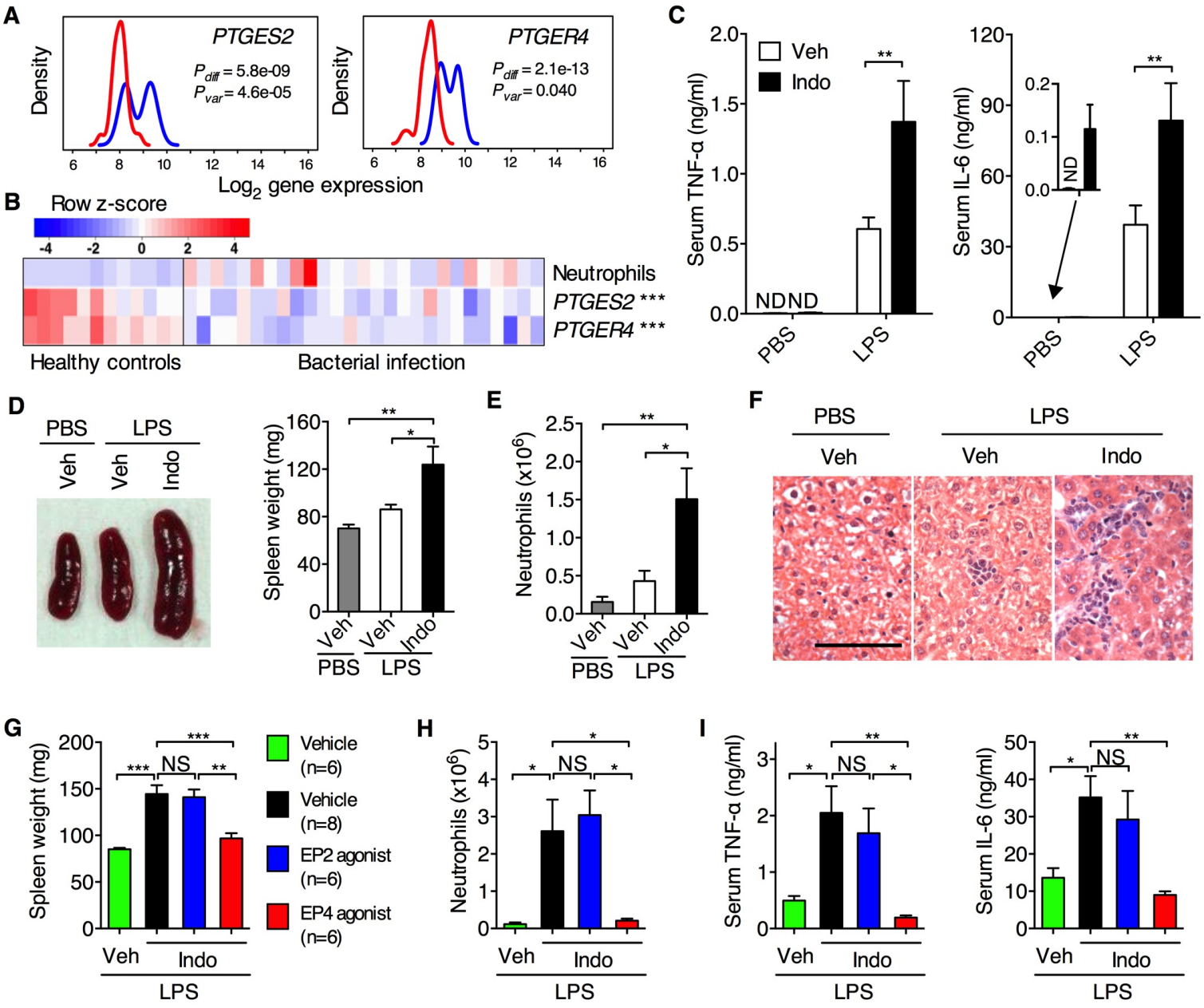
A
PTGES2
P_{diff} = 5.8e-09
P_{var} = 4.6e-05
PTGER4
P_{diff} = 2.1e-13
P_{var} = 0.040
Density
Log2 gene expression
B
Row z-score
Neutrophils
PTGES2 ***
PTGER4 ***
Healthy controls
Bacterial infection
C
Veh
Indo
Serum TNF-α (ng/ml)
Serum IL-6 (ng/ml)
ND
PBS
LPS
D
PBS
LPS
Veh
Indo
Spleen weight (mg)
E
Neutrophils (x10^6)
F
G
Vehicle (n=6)
Vehicle (n=8)
EP2 agonist (n=6)
EP4 agonist (n=6)
NS
H
I

Figure 2

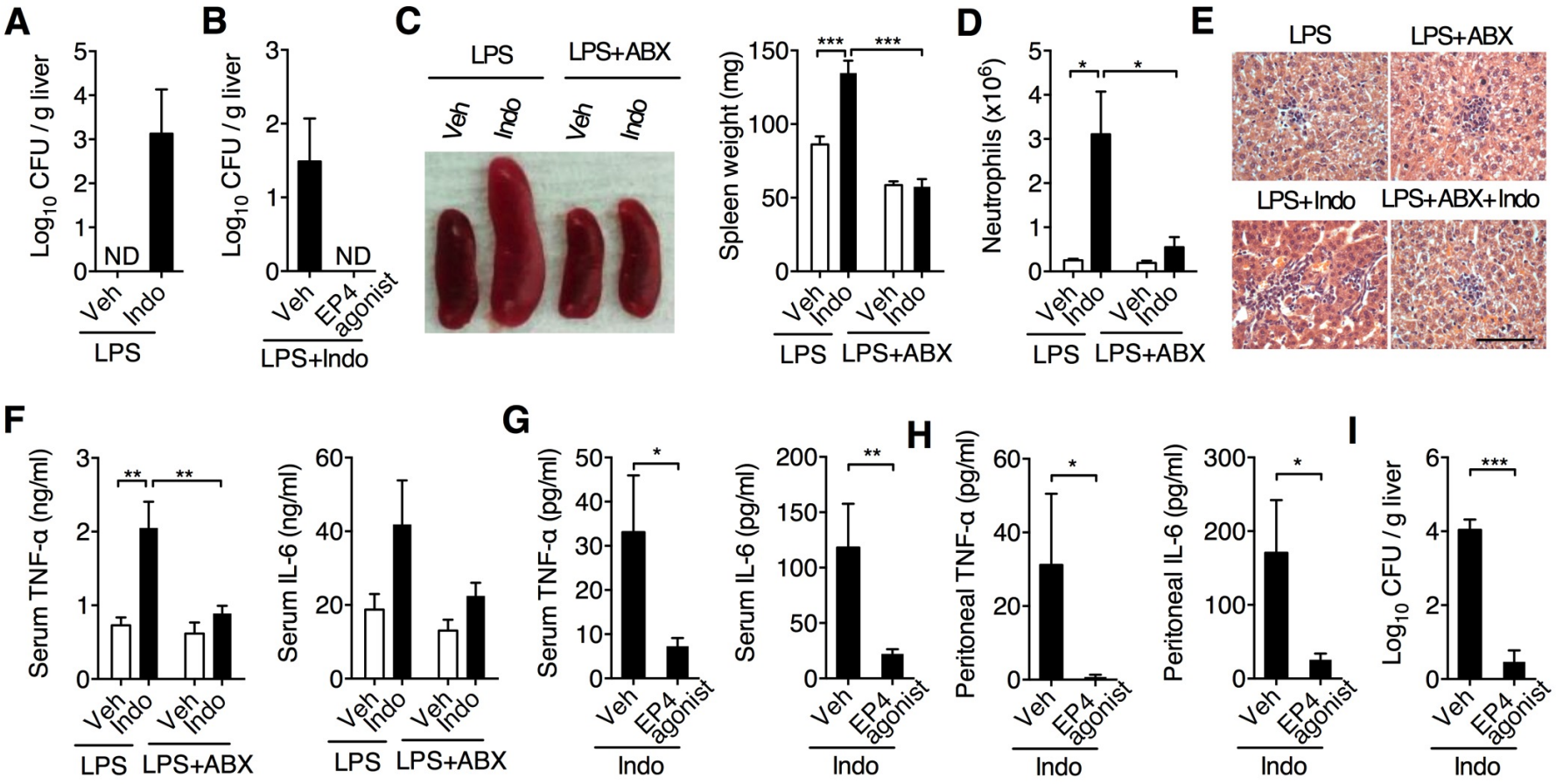
A
Log10 CFU / g liver
ND
Veh
Indo
LPS
B
Log10 CFU / g liver
ND
Veh
EP4 agonist
LPS+Indo
C
LPS
LPS+ABX
Veh
Indo
Veh
Indo
Spleen weight (mg)
***
***
Veh
Indo
Veh
Indo
LPS
LPS+ABX
D
Neutrophils (x10^6)
*
*
Veh
Indo
Veh
Indo
LPS
LPS+ABX
E
LPS
LPS+ABX
LPS+Indo
LPS+ABX+Indo
F
Serum TNF-α (ng/ml)
**
**
Veh
Indo
Veh
Indo
LPS
LPS+ABX
Serum IL-6 (ng/ml)
Veh
Indo
Veh
Indo
LPS
LPS+ABX
G
Serum TNF-α (pg/ml)
*
Veh
EP4 agonist
Indo
Serum IL-6 (pg/ml)
**
Veh
EP4 agonist
Indo
H
Peritoneal TNF-α (pg/ml)
*
Veh
EP4 agonist
Indo
Peritoneal IL-6 (pg/ml)
*
Veh
EP4 agonist
Indo
I
Log10 CFU / g liver
***
Veh
EP4 agonist
Indo

Figure 3

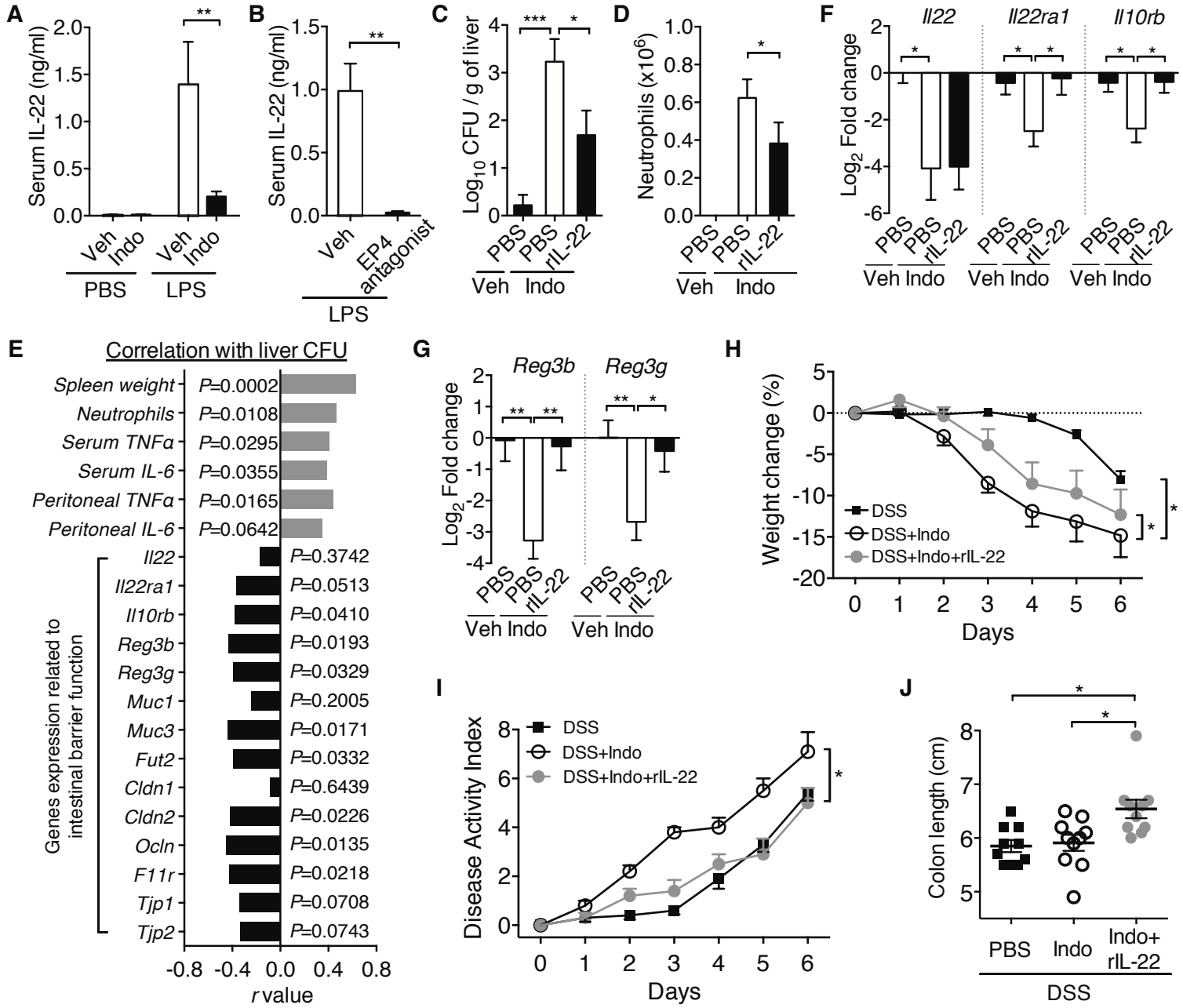
A
Serum IL-22 (ng/ml)
Veh
Indo
Veh
Indo
PBS
LPS
B
Serum IL-22 (ng/ml)
Veh
EP4 antagonist
LPS
C
Log10 CFU / g of liver
PBS
PBS
rIL-22
Veh
Indo
D
Neutrophils (x10^6)
PBS
PBS
rIL-22
Veh
Indo
F
Il22
Il22ra1
Il10rb
Log2 Fold change
PBS
PBS
rIL-22
Veh Indo
E
Correlation with liver CFU
Spleen weight P=0.0002
Neutrophils P=0.0108
Serum TNFα P=0.0295
Serum IL-6 P=0.0355
Peritoneal TNFα P=0.0165
Peritoneal IL-6 P=0.0642
Il22 P=0.3742
Il22ra1 P=0.0513
Il10rb P=0.0410
Reg3b P=0.0193
Reg3g P=0.0329
Muc1 P=0.2005
Muc3 P=0.0171
Fut2 P=0.0332
Cldn1 P=0.6439
Cldn2 P=0.0226
Ocln P=0.0135
F11r P=0.0218
Tjp1 P=0.0708
Tjp2 P=0.0743
Genes expression related to intestinal barrier function
-0.8 -0.4 0.0 0.4 0.8
r value
G
Reg3b
Reg3g
Log2 Fold change
PBS
PBS
rIL-22
Veh Indo
H
Weight change (%)
DSS
DSS+Indo
DSS+Indo+rIL-22
Days
I
Disease Activity Index
DSS
DSS+Indo
DSS+Indo+rIL-22
Days
J
Colon length (cm)
PBS
Indo
Indo+ rIL-22
DSS

Figure 4

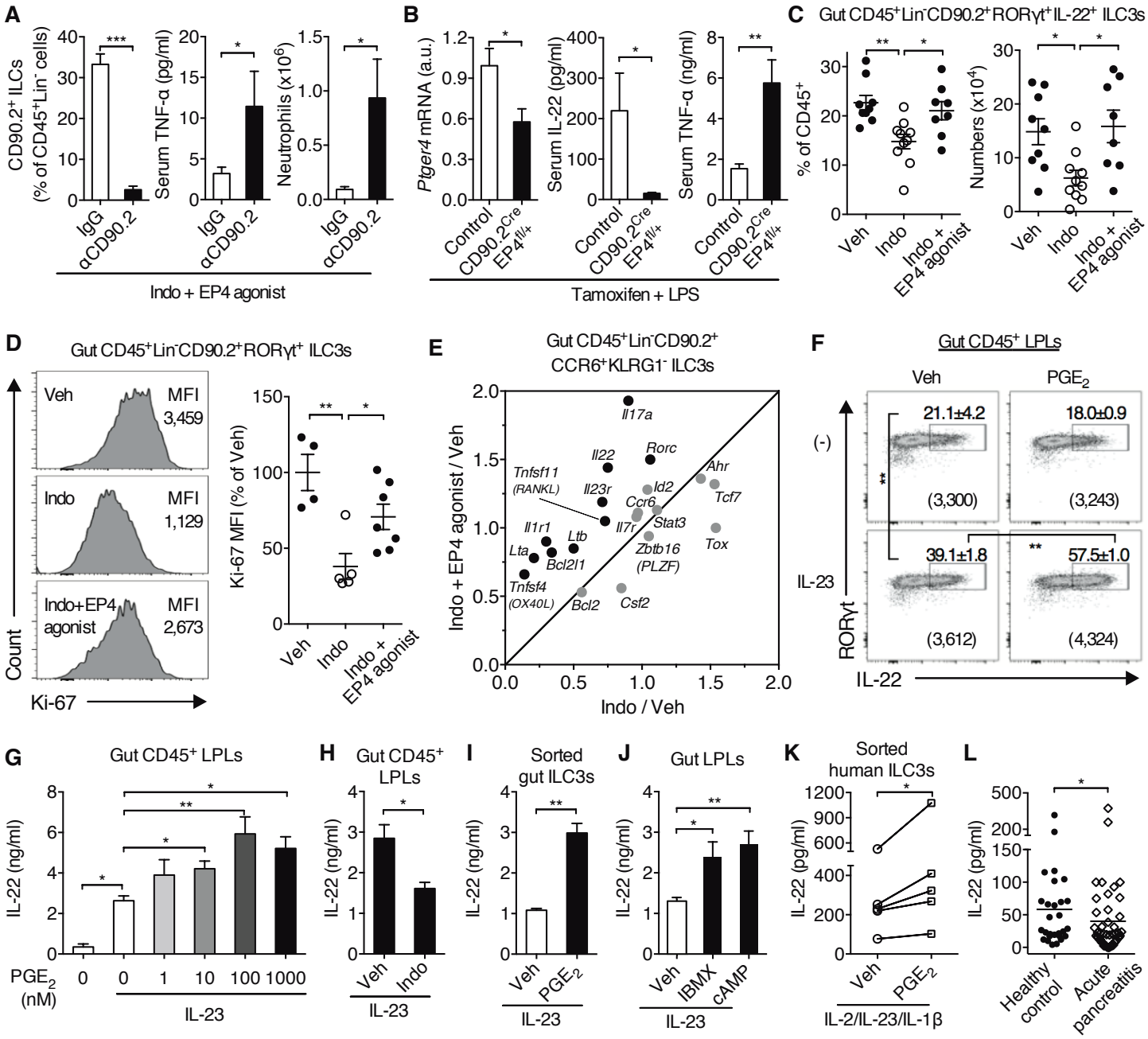
A
CD90.2+ ILCs (% of CD45+Lin- cells)
Serum TNF-α (pg/ml)
Neutrophils (x10^6)
IgG
αCD90.2
Indo + EP4 agonist
B
Ptger4 mRNA (a.u.)
Serum IL-22 (pg/ml)
Serum TNF-α (ng/ml)
Control
CD90.2Cre EP4fl/+
Tamoxifen + LPS
C
Gut CD45+Lin-CD90.2+RORγt+IL-22+ ILC3s
% of CD45+
Numbers (x10^4)
Veh
Indo
Indo + EP4 agonist
D
Gut CD45+Lin-CD90.2+RORγt+ ILC3s
Veh
MFI 3,459
Indo
MFI 1,129
Indo+EP4 agonist
MFI 2,673
Count
Ki-67
Ki-67 MFI (% of Veh)
E
Gut CD45+Lin-CD90.2+ CCR6+KLRG1- ILC3s
Indo + EP4 agonist / Veh
Indo / Veh
Il17a
Il22
Rorc
Ahr
Tnfsf11 (RANKL)
Il23r
Id2
Ccr6
Tcf7
Il1r1
Il7r
Stat3
Ltb
Lta
Zbtb16 (PLZF)
Tox
Bcl2l1
Tnfsf4 (OX40L)
Bcl2
Csf2
F
Gut CD45+ LPLs
Veh
PGE2
(-)
21.1±4.2
18.0±0.9
(3,300)
(3,243)
39.1±1.8
57.5±1.0
(3,612)
(4,324)
IL-23
RORγt
IL-22
G
Gut CD45+ LPLs
IL-22 (ng/ml)
PGE2 (nM)
0
0
1
10
100
1000
IL-23
H
Gut CD45+ LPLs
Veh
Indo
IL-23
I
Sorted gut ILC3s
Veh
PGE2
IL-23
J
Gut LPLs
Veh
IBMX
cAMP
IL-23
K
Sorted human ILC3s
IL-22 (pg/ml)
Veh
PGE2
IL-2/IL-23/IL-1β
L
IL-22 (pg/ml)
Healthy control
Acute pancreatitis